

Statistical properties of the LEDA redshift database

Luca Amendola

Osservatorio Astronomico di Roma, V. Parco Mellini 84, 00136, Roma Italy

Helene Di Nella

Max planck fur Astronomie, Koenigstuhl 17, D69117 Heidelberg, Germany

Marco Montuori and Francesco Sylos Labini

Dipartimento di Fisica, Università di Roma “La Sapienza” P.le A. Moro 2, I-00185 Roma, Italy.

INFM, Sezione di Roma 1

Abstract

We present the statistical properties of large scale galaxy distribution in the LEDA redshift database. This catalog contains more than 40,000 redshifts over all the sky. We find that LEDA, although seriously affected by incompleteness, shows quite stable statistical properties. In particular, we have considered the behaviour of the two points correlation function and of the power spectrum of the density fluctuations, and we have done several tests to check whether the incompleteness of the catalog affect these statistical quantities. Our conclusion is that galaxy distribution in this catalog has fractal properties up to the distance $\sim 200h^{-1}\text{Mpc}$ with $D = 2.1 \pm 0.2$, with no sign towards homogeneity: this result is statistically stable. We analyze also the properties of the angular distributions, finding a complete agreement with the results obtained in redshift space. Finally, we compare these results with those obtained in other redshift surveys, finding that this sample well reproduces the properties of galaxy distribution found in the different catalogs.

1. INTRODUCTION

In the last twenty years there has been a very fast development of the observational techniques in large scale astrophysics. For example, in 1980 only one thousand redshifts of galaxies were known, while now there are available about 50,000 redshifts, and in a few years it is expected that this number will reach about one million. The possibility of studying the large scale structure of the Universe by satellites in various electromagnetic bands (from the microwaves to the γ and X rays) has improved dramatically our knowledge of the Universe. However, despite this observational effort, the most popular theoretical models, and in particular the Hot Big Bang theory and related galaxy formation models, encounter strong difficulties and any new observation requires a new "ad hoc" explanation and, often, the introduction of new free parameters.

One of the main tasks of observational Cosmology is the identification of the homogeneity scale λ_0 above which the distribution of galaxies may really become homogenous (we refer the reader to Davis¹ and Pietronero² for an up to date discussion of the two different point of views on the matter). The present three dimensional data on the distribution of galaxies already gives us the possibility to study and characterize quantitatively the visible matter distribution at least up to $150 \div 200h^{-1}\text{Mpc}$. Among the main features reported in recent years we cite the large void discovered by Kirshner and co-workers³ and an evidence for cell-like structure of the Universe reported by Einasto and co-workers⁴. Subsequently, by using the CfA redshift surveys, it has been confirmed the existence of voids and discovered a filament in the Coma cluster region^{5,6}. These observations, as well as many others, show that the large scale distribution of visible matter is characterized by having strong inhomogeneities of all scales so that the scale of the largest inhomogeneities is comparable with the extent of the surveys in which they are detected⁷⁻⁹.

In order to study the matter, in this paper we analyze the statistical properties of the LEDA (Lyon-Meudon extragalactic database) redshift catalog¹⁰⁻¹². This database was created in 1983, anticipating the growth of the redshift industry of the last decade and pursuing the philosophy of the RC1 and RC2 catalogs, and now contains more than 120,000 galaxies with the most important astrophysical parameters: names of galaxies, morphological description, diameters, axis ratios, magnitudes

in different colors, radial velocities, 21-cm line widths, central velocity dispersions, etc. In the 12 years since the inception of LEDA, more than 75,000 redshifts have been collected, for more than 40,000 galaxies. In this extended galaxy catalog it is possible to identify the main morphological features of galaxy distribution in the Local Universe, i.e. up to $\sim 200h^{-1}\text{Mpc}$, and in particular to study the large scale structure distribution by means of a quantitative statistical analysis, as we are going to show in the following.

In LEDA samples, Paturel and co-workers¹³ identified a very large structure that was called hypergalactic because it seems to connect several superclusters (Perseus-Pisces, Pavo- Indus, Centaurus and The Local Supercluster). Di Nella & Paturel¹⁴ showed that this structure seems to delineate a privileged plane of the Local universe containing 45% of the galaxies where only 25% would be expected if the galaxy distribution was homogeneous. Here we briefly summarize the main morphological features of galaxy distribution in the LEDA catalog.

The usual statistical description of galaxy correlation make use done of the $\xi(r)$ correlation function¹⁵. By analyzing the behavior of this function in the CfA1 redshift survey Davis & Peebles¹⁵ found that galaxy distribution is characterized by having a well defined "correlation length" of $r_0 \approx 5h^{-1}\text{Mpc}$. In this interpretation, this length should be a physical characteristic scale, and galaxy distribution should be homogeneous at a few times r_0 i.e. $\sim 15 \div 25h^{-1}\text{Mpc}$. However from the simple visual inspection of redshift maps of galaxies one can see that there are inhomogeneities of one order of magnitude larger than r_0 (for example the Great Wall has an extension of $\sim 170h^{-1}\text{Mpc}$ ¹⁶), and hence this statistical analysis seems to give an inconsistent result. How can a correlation length of $5h^{-1}\text{Mpc}$ be compatible with the existence of large scale structure of $150h^{-1}\text{Mpc}$?

In order to clarify this fundamental problem, Pietronero and co-workers¹⁷⁻¹⁹ introduced a new statistical analysis that reconciles galaxy correlation with the existence of LSS. This correlation analysis, well known and used in other field of Physics such as Statistical Mechanics, is appropriate for studying highly irregular distributions, but, of course, it can be successfully applied also in the case of smooth (homogenous) distributions. The new analysis performed by¹⁹ showed that the interpretation of the standard analysis performed using the $\xi(r)$ two-points correlation function¹⁶ is based on the

assumption that the sample under analysis is homogeneous. In the case in which this basic hypothesis is not satisfied the $\xi(r)$ analysis gives misleading results because it gives information that are related to the sample size rather than to any real physical features. For example, Coleman & Pietronero¹⁹ found a fractal behaviour in the CfA1 redshift survey up to $\sim 20h^{-1}\text{Mpc}$ with a fractal dimension $D \approx 1.5$. This result implies that the correlation length r_0 defined by $\xi(r_0) = 1$ is spurious, and does not correspond to any real feature of galaxy distribution, but instead it is related to the size of the sample analyzed.

Sylos Labini *et al.*²⁰ found that in Perseus-Pisces surveys the fractal behaviour extends up to $130h^{-1}\text{Mpc}$ with $D \approx 2$. Moreover in Pietronero *et al.*² (see for a review Sylos Labini *et al.*²¹) we have analyzed the behavior of the correlation function for all the published redshift surveys (SSRS, CfA, IRAS, Stromlo-APM, LCRS, ESP and also some cluster catalogs) finding that all the available samples show fractal correlation with $D \approx 2$ up to limit of the statistical validity ($\sim 150h^{-1}\text{Mpc}$), without any tendency towards homogenization. In the case of ESP, the fractal behavior extends to $\sim 1000h^{-1}\text{Mpc}$; however, in this case, the analysis is made difficult because it requires K -corrections, the adoption of a cosmological model, and a modeling of evolutionary effects.

Here we investigate the correlation properties and the power spectrum of the redshift samples available in LEDA database. By the full correlation analysis of volume limited (hereafter VL) samples, we are able to extend the behavior of the two points correlation function up to $\sim 150h^{-1}\text{Mpc}$. This is the only galaxy catalog currently available in which it is possible to study the correlation function for three decades of distances. We find that, in this range of scale, galaxy distribution is well represented by a fractal distribution with $D \approx 2$.

Moreover we consider the power spectrum (PS) of the density fluctuations. This is one of the most popular and useful ways to characterize a distribution. In astrophysics the power spectrum is particularly significant because most models of primordial galaxy formation predict a specific spectrum shape; in the gravitational linear theory, different k -modes evolve independently, so that the present power spectrum carries direct information on the primordial physical processes that generated the fluctuations. However even the determination of the PS is based on the assumption of the existence of

a well defined average density. Currently, the observations allow one to compute the *luminous matter* power spectrum on small and intermediate scales, say up to $\approx 200h^{-1}\text{Mpc}$, through the mapping of the local galaxy clustering, and the *gravitational matter* power spectrum on large scales ($> 1000h^{-1}\text{Mpc}$), mainly through investigation of the microwave background anisotropies. One of the most extended redshift surveys, the CfA2 survey ²² presents a power spectrum rising with the scale $\lambda = 2\pi/k$ at large wavenumbers as $P \sim k^{-2}$, and flattening around $150h^{-1}\text{Mpc}$. These features are also confirmed by the SSRS2 data ²³. Other authors find similar trends ^{24–27,56} although with some differences on the location of the flattening and on the overall amplitude.

The flattening is usually interpreted as the convergence to homogeneity of the sample, reminiscent of the flattening to a vanishing value of the correlation function on scales $> 30h^{-1}\text{Mpc}$ ^{28,22} and of the angular correlation function at separations $> 10^0$ ²⁹. However, all these surveys, when cut in volume limited subsamples, extend to no more than $130 h^{-1}\text{Mpc}$ (in CfA2 ²²). The fact that the flattening occurs just around this scale should prompt a more cautious investigation (see remarks in da Costa et al. ²³).

An even stronger caution should be exerted as one observes that the amplitude of the power spectra seems to depend on the sample size. From CfA101 to CfA130²² (PVGH), for instance, the spectrum amplitude increases by 40%. Two explanations have been proposed so far for the scaling: luminosity biasing and sampling fluctuations. The effect of luminosity biasing, however, is found to be insufficient by the same CfA2 authors (PVGH, see their Fig. 11a) at least on these scales, and by the Las Campanas authors ⁵⁶. The second explanation, sampling fluctuations, is unlikely, in our opinion, for two reasons. First, if the survey reached the homogeneity scale, the distribution statistics must approach the Poisson distribution. Then, in a survey with N galaxies, the sampling fluctuations go roughly as \sqrt{N} : both in the CfA2 and in the LCRS case, this amounts to fluctuations of the order of a few percent, certainly not enough to explain the strong trend in the PS. Secondly, even if the fluctuations were strong enough, there is no reason to expect the *systematic* scaling reported in CfA2 and LCRS. Therefore, in the standard context, in which the inhomogeneities are not supposed to extend to very large scales, such a scaling is so far unexplained. In Sylos Labini & Amendola ³⁰ a

different explanation, based on a fractal viewpoint¹⁹, was instead proposed: a finite portion of a fractal shows indeed the same kind of flattening and scaling as reported in CfA2. Both features appear then a mere consequence of the finiteness of the sample. The scale of homogeneity, if this interpretation is correct, is then pushed longward of $150h^{-1}\text{Mpc}$.

In order to investigate further this important question, a very large and deep database is needed. In fact, to minimize the effects of the window filtering in the PS calculation, a large sky coverage is necessary. In this paper we attempt a determination of the PS in the LEDA database extending from a few Megaparsecs to more than $150 h^{-1}\text{Mpc}$. This is the most extended galaxy PS so far obtained in literature. On the largest scales, the effects of poor sampling can be significant; we will be cautious in deriving too strong conclusions from our data. Nevertheless, the picture we obtain is amazing: no sign of convergence to homogeneity is reached; no deviation from a fractal dimension $D \approx 2$ is detected; and, finally, no reasonable CDM-like fit seems possible on our deepest PS. If these results will be confirmed by more complete surveys, some radical change in our view of the galaxy clustering should be adopted.

We would like to stress that we have done several tests, both for the space correlation and for the power spectrum analysis, in order to check the stability of the results versus the possible incompleteness of the sample (see the remarks in Davis¹). We find that this survey, although it is strongly affected by incompleteness, show a quite stable statistical signal.

A part the direct three dimensional correlation analysis, that is clearly the most appropriate way to study the statistical properties of galaxy distribution, it has been claimed^{31,1} that there are some indirect evidences, based on the angular properties, that points towards an homogenous galaxy distribution. In order to understand the properties of the angular distribution, in Sylos Labini *et al.*³² we have introduced and studied two new concepts, *the dilution effect* and *the small scale fluctuations*, which are essential for the quantitative analysis of the statistical validity of the available galaxy samples. We show that the various data that are considered as pointing to a homogeneous distribution are all affected by these spurious effects and their interpretation should be substantially changed. In this paper we present also several tests on the angular distributions. In particular, we study the behaviour

of the galaxy number counts. The angular data have clearly less information, with respect to the three dimensional ones, and must be studied with great caution. However, we find even in this case a complete agreement with the fractal picture.

2. THE SAMPLE

LEDA is an all-sky catalog, containing more than 40,000 redshifts. The data of the galaxies recorded in the LEDA database come from many different references from the literature. The major problems concern the reduction of the apparent magnitudes of galaxies, as well as other parameters, in an homogeneous system, and the quantification of the incompleteness due to the different sampling ratio in different area of the sky.

Paturel and co-workers ¹⁰ have done a detailed study on the apparent magnitudes, and they have given the formulae to reduce twenty different magnitudes systems to the photoelectric B_t system of the Third Reference Catalogue (RC3). This reduction is done in such a way that the resulting magnitudes are completely free of bias or perturbing effects. Each magnitude is then given with its own error. This error is of course in the range 0.1 to 1 magnitude depending of the observations and of the comparison between different published values for the same galaxy. The major part of the galaxies have a mean error less than 0.5 magnitude. The complete list of the references of the magnitudes used in LEDA is available on the net ^{11,12} (we refer to this paper also for more information of the data contained in LEDA).

The main selection effect that must be studied with great care is the incompleteness of the redshift data available in the LEDA database for different directions of observation. The sampling ratio is different in different angular regions.

In Fig.1 we report the percentage of galaxies known in angular catalogs compared to the number of galaxies having a measured redshift. One can see that up to the limiting magnitude $B_t = 14.5$, LEDA have a rate of redshift measurements of 90%, if we extend the study by including fainter galaxies up to a limit of $B_t = 16$, this rate falls to 60%, and with $B_t = 17$, LEDA has only redshift for 50% of these galaxies. However the absolute sampling ratios, i.e. the fraction f of galaxies with measured redshift

versus the total number of galaxies present in the sky up to a certain apparent magnitude limit (and not only the galaxies with measured angular properties) is $f \approx 0.9$ for $B_t = 14.5$, $f \approx 0.5$ for $B_t = 16$, and $f \approx 0.1$ for $B_t = 17$.

In order to investigate the incompleteness of the LEDA database we have built two magnitude limited (ML) samples: the first is limited at $m = 14.5$, is complete to 90%, and it is called LEDA14.5, the second is limited at $m = 16$ (completeness 50%, LEDA16). Further, to compare the PS with the results from CfA, we extracted another catalog, cut to reduce it to the CfA-North boundaries (R.A. $8^h < \alpha < 17^h$, declination $8.5^0 < \delta < 44.5^0$, with a further cut to reduce galactic obscuration, see PVGH), to be denoted as Leda-CfA . This sample contains 4593 galaxies in an angular area of 1.23 sr, amounting to a completeness level of 70% (infact, CfA2 North contains in this region 6316 galaxies, see PVGH).

The problem that we will discuss in detail is whether the incompleteness in the deeper samples destroys the statistical relevance of these samples, or whether it is possible to recover the right statistical properties and to control the effects of such incompleteness. In particular we will do several quantitative tests to clarify this crucial point. In order to avoid the zones of avoidance due to the Milky Way, we cut the all-sky samples in the half-skies catalogs. In this way we will have for example, LEDA14.5N that refers to the northern hemisphere, and LEDA14.5S that refers to the southern one. The samples denominated North and South in the paper are respectively selected with the galactic latitude: $b > +10^\circ$ and $b < -10^\circ$, as usually done in literature. We correct the velocity for the heliocentric motions, and we use the Local Group reference frame (see for example Park et al.²²). The Hubble constant is $H_0 = 100h \cdot kmsec^{-1}Mpc^{-1}$.

We have then 5 ML samples: LEDA14.5N and LEDA14.5S, LEDA16N and LEDA16S, and LEDA-CfA. We will analyzed separately each of these samples. Moreover to perform the space distribution analysis we extract various volume limited (VL) samples and we report in followings their characteristics. In such a way we have various independent VL samples, and we will analyze in the following the statistical properties of all these subsamples.

In Tab.I we show the characteristics of the VL samples extracted from the database limited at the

apparent magnitude 14.5 (LEDA14.5N), in the same sky region of CfA1.

In Tab.II we show the properties of the VL samples (limited in absolute magnitude) extracted from the database limited at 14.5. The parameter p is defined in section 4.

Tab.III is the same as Tab.II for the database limited at the apparent magnitude 16 (LEDA16N and LEDA16S).

3. MORPHOLOGICAL PROPERTIES OF THE SPATIAL DISTRIBUTION OF GALAXIES

In the following we describe, how we obtain the largest three dimensional maps of the distribution of galaxies. From the simple visual inspection of angular distributions, one can see that galaxies are not randomly distributed but that they are merged in clusters and large structures of several tens of megaparsecs. It is already known, after de Vaucouleurs studies ^{33,34}, that nearby galaxies form a flat structure, the Local Super cluster, the pole of which is defined by galactic coordinates $l = 47$ deg; $b = 6$ deg.

In 1988, Geller and Huchra ³⁵ showed that the Coma filament was indeed a sheet-like structure, the so-called *great wall*, similar to structures predicted by a model due to Zeldovich ³⁶. In the southern hemisphere, another remarkable work was done by Da Costa *et al.* and Fairall *et al.* ^{37,38} who exhibited another wall-like structure in the Pavo-Indus region. On the other hand, the Perseus-Pisces region was described as a chain ³⁹ or sheet-like structure ⁴⁰.

Paturel and co-workers ^{41,13} (see Fig.2) discovered a very large structure that seems to connect several superclusters (Perseus-Pisces, Pavo-Indus, Centaurus and The Local Supercluster, that was called hypergalactic plane (to not refer to the orientation of the supergalactic system, i.e. our Local Supercluster).

The pole of this hypergalactic structure was about $l = 57$ deg; $b = 22$ deg in galactic longitude and latitude respectively.

In order to study the three dimensional features of such a structure, from the LEDA database, we have built a sample of 24,324 galaxies with radial velocities smaller than $15,000 km.s^{-1}$. For a plane defined by the coordinates of its pole lp and bp (galactic longitude and latitude, respectively),

we counted the number of galaxies which are lying in a conic zone of ± 15 deg on each side of the plane. We computed a systematic research of the most populated plane, by giving values between 0 to 90 deg for b and between 0 to 360 deg for l .

One can see in the Tab.IV the result of this galaxy count: d is the limiting distance of the counting (given in Megaparsec), N_{gal} is the total number of galaxies within this limit, lp and bp are the galactic coordinates which define the most populated plane and $\%_{gal}$ is the percentage of galaxies which are lying within ± 15 deg of the previous plane. If the galaxies were uniformly distributed in the sphere of computation of radius d , when looking in a zone of 30 deg, i.e. in a solid angle of π steradians, one should find 25% of the total number of galaxies within the sphere.

A position of the pole at $lp = 52$ deg; $bp = 16$ deg seems particularly stable between 80 Mpc and 200 Mpc. This pole is similar to the one given in 1988. It will be used to define the hypergalactic coordinates hgl , hgb . From the Tab.IV it is also possible to give a new determination of the pole of the Local Supercluster plane. In 1976 de Vaucouleurs gave: $lp = 47$ deg and $bp = 6$ deg for the galaxies up to about $3,000 \text{ km.s}^{-1}$, here we find $lp = 46$ deg and $bp = 14$ deg, for the same region, which is in very good agreement.

We show in Fig.3 the map of the three dimensional galaxy distribution in hypergalactic coordinates.

The origin of hypergalactic longitudes is arbitrarily defined as $l(origin) = l(pole)$ and $b(origin) = b(pole) - 90$ deg. The Cartesian XYZ - coordinates are thus calculated from hypergalactic longitude and latitude, hgl and hgb respectively, using the following equations:

$$X = r \cdot \cos(hgb) \cdot \cos(hgl) \quad (1)$$

$$Y = r \cdot \cos(hgb) \cdot \sin(hgl) \quad (2)$$

$$Z = r \cdot \sin(hgb) \quad (3)$$

where r is the distance deduced from the radial velocity assuming the Hubble constant to be $H_o = 75 \text{ km.s}^{-1} \cdot \text{Mpc}^{-1}$.

One should notice from this representation of the galaxy distribution;

- Some radial structures at the periphery are very elongated. These structures are due to the uncertainties on the distance deduce from the radial velocity. As a fact the radial velocity measured is not only the cosmological velocity (as a function of the distance). The radial component of the velocity dispersion of the galaxies in a cluster is superimposed to this cosmological velocity. It then appears a dispersion on the distances, although *quasi* no error exists in direction. Hence the clusters appear elongated along the line of sight. All these clusters seems to point toward our Galaxy: this effect is known as the "fingers of god". Some methods exist to correct for such an observational effect, however in the present studies we didn't use them, in order to not add any not well controlled effect. This implies that one should not give too much signification to any radial structure which could be due to this artifact.
- One can see a zone (vertical on the plot X-Y) where no galaxy appear. This zone results from the absorption due to the dust of the disk of our Galaxy, which hide the others galaxies of the Universe in this direction. One should hope that the surveys in the infrared with spectroscopic follow-up will solve this problem.
- The most interesting result visible on Fig.3 is the empty region surrounding the Local Supercluster (centered on Virgo cluster), delimited by a belt of neighbor Superclusters: Perseus-Pisces, Pavo-Indus, Centaurus and the Great Wall. All these structures seem to be curved towards the direction of the Local Supercluster (LSC) and being located at a mean distance of 70 Mpc from the LSC. One can't argue that this situation is due to the previous artifact as this effect is not radial. A perpendicular projection to the hypergalactic plane (Fig.4) shows that this tendency is three-dimensional as the Great Wall is actually curved in the direction of the LSC.

From the previous sample of galaxies limited in apparent magnitude to $B_t < 14.5$, we constructed volume limited samples with the standard procedure ^{16,19}. We then compute the research for a privileged plane with this different subsamples. The results are given in Table..

The pole of the Local Supercluster ($d < 20$ Mpc) is found close to the published value by De Vaucouleurs in the RC2 ($l=47\text{deg}$, $b=6\text{deg}$) with 57% of galaxies of the sample located in the region of

+/- 15 deg of the plane. On large scale the hypergalactic plane is present with roughly 40% of the galaxies in the region of +/- 15 deg of the plane. The value of its pole is very close to the one found with the galaxy sample limited in apparent magnitude to $B_t < 14.5$.

4. THREE DIMENSIONAL CORRELATION FUNCTION

With the aim of performing an analysis that does not require any a priori assumption on the nature of the galaxy distribution in our samples, we have computed the conditional density $\Gamma(r)$ ¹⁹. The function $\Gamma(r)$ measures the conditional density inside a spherical shell of thickness Δr at distance r from an occupied point. Having a three dimensional sample with N galaxies, one can measure the $\Gamma(r)$ function from all the points of the sample, and then one performs the average:

$$\Gamma(r) = \frac{1}{N} \sum_{i=1}^N \frac{1}{4\pi r^2 \Delta r} \int_r^{r+\Delta r} n(\vec{r}_i + \vec{r}) d\vec{r} = \langle n(r_i + r) \rangle_i \quad (4)$$

where $n(\vec{r})$ is the density at \vec{r} and the final average $\langle \dots \rangle_i$ refers to all the occupied points r_i . The exponent of $\Gamma(r)$ is therefore a global property of the system and it is a robust statistical quantity. We will prove this statement with specific tests in the following. It is useful to introduce the average conditional density

$$\Gamma^*(r) = \frac{3}{4\pi r^2} \int_0^r \Gamma(r') 4\pi r'^2 dr' \quad (5)$$

to smooth out the small fluctuations of the $\Gamma(r)$ function.

For a fractal distribution the integrated number of points in a sphere around an arbitrary occupied point scales as⁴²

$$N(< r) = Br^D \quad (6)$$

where D is the fractal dimension and B is related to the lower cutoffs of the structure^{19,32}. The average density inside a spherical sample of radius R_s is clearly

$$\langle n \rangle = \frac{3B}{4\pi} R_s^{D-3} \quad (7)$$

In this case it is simple to show that $\Gamma(r)$ (and $\Gamma^*(r)$) will follow a power law behavior as a function of the distance

$$\Gamma(r) = \frac{BD}{4\pi} r^{D-3} \quad (8)$$

If the system is homogenous the conditional density is clearly flat ($D = 3$), so that this statistical tool is the appropriate one to study the fractal versus homogeneity properties. It is simple to show that in the case of a fractal with dimension D the conditional average density is $\Gamma^*(r) = (3/D)\Gamma(r)$.

It is important to recall here that the conditional density is computed in spherical shell, and in a certain catalog, the maximum depth up to which it is possible to compute $\Gamma(r)$ is of the order of the radius of the maximum sphere fully contained in the sample volume ^{19,21}. This length is determined by both the depth of the sample and by its solid angle in the sky.

Before preceding, it is important to remark a fundamental point. The main point of the LEDA database analysis is that from the law of codimension additivity ³² it follows that if we cut points randomly from a fractal distribution, its fractal dimension does not change. To clarify a point that became essential in the following analysis, we discuss briefly the law of codimension additivity ^{42,19}. This states that the dimension D_I of the intersection of two objects with dimension d_A and d_B embedded in a space with dimension d is

$$D_I = d_A + d_B - d \quad (9)$$

For example if $d_A = D$ is the fractal dimension of galaxy distribution (in the three dimensional Euclidean space $d = 3$), and we intersect it with random distribution $d_B = 3$, i.e. we cut points in a random manner, we have that $D_I = D$. Hence, if we cut points randomly from a fractal distribution, its fractal dimension does not change. The cutting procedure can be applied up to eliminate the $\sim 96 - 98\%$ of the points of the structure without changing the genuine properties of distribution ³².

It is clear that if the incompleteness effects are randomly distributed in space, they will not affect the correlation properties of the sample, unless the percentage of the points present in the sample is so small that the sampling noise dominates. On the contrary if there are some systematic effect, as a poor sampling in certain regions, the correlation properties can be seriously affected.

To select the *statistically fair samples*, i.e. the VL samples that contain enough points to allow one to recover the correct statistical properties of the distribution from which it has been extracted (see Sylos Labini *et al.*³²), we should firstly determine the percentage of the total number of points present in these samples with respect to an ideal complete survey. This can be done knowing the value of the lower cut-off B (Eq.(6)) of the fractal structure. We can compute the fraction of the points present in the sample computing the apparent lower cut-off B_a

$$B_a = \frac{4\pi N_a}{\Omega R^D} \quad (10)$$

where N_a is the number of points present in the VL sample, Ω is the solid angle of the survey and R is the depth of the VL sample considered. Then the percentage of points is

$$p = \frac{N_a}{N} = \frac{B_a}{B} \quad (11)$$

where N is given by Eq.(6). To compute the *absolute* lower cut-off B , it is possible to compute the amplitude of $\Gamma(r)$ in a VL sample, and then normalize it to the luminosity selection effect that sample. We have computed it in several VL samples of Peruses-Pisces and CfA1³² and we have found that $B \sim 15(h^{-1}Mpc)^{-D}$. We will adopt this value in the following calculations. We list in the Tables 1-2 the characteristics of the VL samples used, with the relative percentage. We have checked that if the percentage is lower than $\sim 1 \div 2\%$ the correlation properties are destroyed (see Sylos Labini *et al.*³²). Hence the VL samples that we use, have the characteristic to be *statistically fair samples*. The analyses presented here concern only the samples for which $p \gtrsim 2\%$.

The amplitude of $\Gamma(r)$ is related to the lower cut-offs of the distribution and it is simply connected to the prefactor of the average density (Eq.(8)). To normalize the conditional density in different VL samples (defined by the absolute magnitude limit M_{lim}) we divide it by the Luminosity Factor:

$$\Phi(M_{lim}) = \int_{-\infty}^{M_{lim}} \phi(M) dM \quad (12)$$

where $\phi(M)$ is the Schechter luminosity function³². As parameter of $\phi(M)$ we adopt $\delta = -1.1$ and $M_* = -19.7$ ⁹. The normalized CF is

$$\Gamma_n(r) = \frac{\Gamma_{M_{lim}}(r)}{\Phi(M_{lim})} \quad (13)$$

where $\Gamma_{M_{lim}}(r)$ is the usual CF expressed by Eq.(8).

In order to control the effect of the incompleteness in the data, we have firstly studied the correlation properties of the two VL samples extracted from LEDA14.5. These samples are nearly complete, and the incompleteness is no more than $\sim 10\%$. To compare our results with other published we have computed the correlation function in the same region of the CfA1 redshift survey. In this case we have a complete sample because LEDA contains the CfA1 redshift catalog. We find that the number of points in the various VL sample of LEDA14.5-CfA1 are nearly the same of that of CfA1. The conditional density scales as a power law with $\gamma = 3 - D = 0.9 \pm 0.2$ ($D = 2.1 \pm 0.2$) up to the sample limit that is $\sim 20h^{-1}\text{Mpc}$. The results of our analysis are therefore in perfect agreement with those of CfA1^{19,21}.

The next step is to increase the solid of angle of the LEDA14.5N up to include all the northern hemisphere. We find that the CF function does not change its slope nor its amplitude, so that it remains a power law with the same fractal dimension. The scaling region extends up to $\sim 30h^{-1}\text{Mpc}$. Therefore in this way we can control the effect of incompleteness and conclude that this result confirms that the small incompleteness of this sample does not affect the correlation properties of galaxy distribution.

We have done the same analysis for the VL samples of LEDA14.5S finding a result in substantial agreement with that of LEDA14.5N. This implies that the statistical properties of the LEDA14.5 are robust with respect to the small incompleteness in the galaxy redshifts that characterize this sample. The fractal dimension in the VL sample of LEDA14.5 turns out to be $D = 2.1 \pm 0.2$.

In Fig.5 there are plotted also the different $\Gamma(r)$ for the various VL samples of LEDA14.5: we find that there is a nice matching of the amplitudes and slopes. This implies that we are computing the correct galaxy number density in each subsample, and that this average density does not depend (or it depends very weakly) on the absolute magnitude of galaxies. We have done this kind of analysis for the whole north galactic hemisphere (LEDA14.5N) and for the southern one (LEDA14.5): in both cases we obtain the same kind of behaviour for $\Gamma(r)$.

The following step is to analyze the VL samples of LEDA16 (north and south). We have studied the behavior of the correlation function $\Gamma(r)$ in the various VL samples of LEDA16N and LEDA16S.

We find in both case the distribution has long-range correlation with the same fractal dimension $D = 2.1 \pm 0.2$, up to $\sim 80 - 90h^{-1}\text{Mpc}$ (Fig.6). In some VL samples of LEDA16 $\Gamma(r)$ we find indeed a minor deviation from a single power law that can possibly be attributed to incompleteness. Such a conclusion is supported also by the Power spectrum analysis (see Sec.7).

To compare the amplitude of $\Gamma(r)$ in the different samples of LEDA16, we consider the normalized CF (i.e divided by the luminosity factor). We find that the amplitude of the normalized CF is about the 40% of that found for LEDA14.5. This is because in this case the sampling rate is not 90% as it is for LEDA14.5 but it is about 50% as we have discussed previously. Hence a part this factor, we have that the CF has the same features of that of LEDA14.5. Even in this case we conclude that the incompleteness present in this sample is randomly distributed in the sky, and the correlation properties are only weakly affected by it.

We have performed another test in order to check the effects of the incompleteness. We have cut a VL sample in two regions, say one up to $50h^{-1}\text{Mpc}$ and the other extending from 50 to $100h^{-1}\text{Mpc}$. We then compute $\Gamma(r)$ in these two subsamples, and we find that same power law behaviour extending on all scales, up to the effective depth of the samples (see Fig.7).

This test shows that the correlation properties of the nearby sample are the same as the deepest one, and that the signal is stable. This behaviour is expected in a fractal distribution, and is contrary to what one has in the case of a radial incompleteness, where the nearby points and the far away ones have different environments. We can conclude again that the incompleteness of the sample does not change the genuine behaviour of the conditional average density.

We have performed also another test: we have cut one sample of LEDA14.5N and one of LEDA14.5S at the limiting magnitude $M = -19$. Then we have measured $\Gamma(r)$: we find the same power law behaviour in these two cases, and also the amplitudes match quite well. Then we have repeated the same procedure with LEDA16, multiplying the amplitude of $\Gamma(r)$ by 0.5/0.9. In such a way we have obtained 4 samples, all with the same magnitude limit $M = -19$: we find that all the amplitudes match quite well, confirming again the statistical stability of the catalog.

As long as the space and the luminosity density can be considered independent, the normalization

of $\Gamma(r)$ in different VL samples can be simply done by dividing their amplitude by the corresponding luminosity factor. Of course such a normalization is parametric, because it depends on the two parameters of the luminosity function δ and M^* ⁴³. For a reasonable choice of these two parameters we find that the amplitude of the conditional and radial density match quite well in different VL samples. We show in in Fig.8 the results of such normalization.

5. STANDARD CORRELATION ANALYSIS

To clarify the basic aspect of the standard analysis we have computed the standard two points correlation function $\xi(r)$ defined as¹⁶

$$\xi(r) = \frac{\langle n(\vec{r}_0)n(\vec{r}_0 + \vec{r}) \rangle}{\langle n \rangle^2} - 1 \quad (14)$$

This function is not suitable to study systems characterized by long-range correlations, as it is widely discussed in Coleman & Pietronero¹⁹. Suppose we have a spherical sample of radius R_s and that the distribution is fractal. Then, the conditional density has a power law behavior, while it is simple to show that

$$\xi(r) = \frac{\Gamma(r)}{\langle n \rangle} - 1 = \frac{D}{3} \left(\frac{r}{R_s} \right)^{D-3} - 1 \quad (15)$$

so that its amplitude *depends* on the sample size R_s and it is not a power law. In particular the standard definition of "the correlation length" $\xi(r_0) = 1$ does not define a real physically meaningful quantity, but is just a fraction of the sample size

$$r_0 = \left(\frac{D}{3} \right)^{\frac{1}{3-D}} R_s \quad (16)$$

Coleman & Pietronero¹⁹ have found the linear dependence of r_0 on R_s in the CfA1 catalog. Here we will check this behavior for all the VL samples that we have built.

In order to measure $\xi(r)$, we have adopted the same procedure used for the computation of $\Gamma(r)$. In fact we have firstly used the VL samples of LEDA14.5-CfA1, to compare the result with those of CP92. Then we have extended the analysis to the whole northern and southern hemispheres. Applying

the same step to LEDA16, we find that in the deeper VL sample r_0 reached the value of $45 \pm 5h^{-1}\text{Mpc}$ for a value of $R_{eff} \approx 150h^{-1}\text{Mpc}$ scaling as a linear function of the sample size Fig.9.

This shows again that the usual $\xi(r)$ is completely misleading if applied to systems characterized by long-range correlations. The so-called "correlation length" r_0 is just an artifact due to an inconsistent mathematical analysis. Being only a fraction of the sample size, it has no physical meaning.

Let us note that $\xi(r)$ is not a power law for a fractal distribution, but it exhibits a break due to the "-1" term. This means that in a log-log plot there is a very sharp break when $r \rightarrow r_0$ because beyond this $\xi(r)$ becomes negative. As a consequence, the function $\xi(r)$ is systematically steeper than the function $\Gamma(r)$ or $1 + \xi(r)$, unless one fits at very small values of r , i.e. at $r \ll r_0$, which is not usually done. The fractal dimension is then usually underestimate ²¹.

6. INTEGRAL FROM THE VERTEX

Let us consider now the conditional average as *observed from the observer*. In order to discuss this question it is important to focus on the role of the *small scale fluctuations*. We have studied in detail the general problem in Sylos Labini et al. ^{32,21} and we refer to these papers for a more complete discussion of the matter.

Considering the conditional average as *observed from the vertex* $n(r) = N(< R)/V(R)$, we expect (Fig.3 - insert panel) that for very small distances we observe essentially no other galaxy, and only at a distance ℓ_v we begin to observe some other galaxy. For distances somewhat larger than ℓ_v we expect therefore a raise of the conditional density because we are beginning to have some points. It is therefore important to be able to estimate and control the *minimal statistical length* λ . In the paper Sylos Labini *et al.*³² we have discussed in detail the effects of the finite size fluctuations, and here we present a new argument for the derivation of the length λ . At small scale, where there is a small number of points, there is an additional term, due to shot noise, superimposed to the power law behaviour of $n(r)$, that destroys the genuine correlations of the system. Such a fluctuating term can be cancelled out by making an average over all the points in the survey. On the contrary, in the observation from the vertex, only when the number of points is larger than, say ~ 30 then the shot

noise term can be not important. This condition gives

$$\lambda = 5 \left(\frac{4\pi}{Bp\Omega} \right)^{\frac{1}{D}} \approx \frac{20 \div 60 h^{-1} \text{Mpc}}{\Omega^{\frac{1}{D}}}. \quad (17)$$

for a typical VL sample with $M_{VL} \approx M^*$, where B corresponds to the amplitude of the conditional density of all galaxies^{32,21}. This can be estimated from the amplitude of the available samples divided by p as defined in Eq.(8). This leads to an estimate (for typical catalogues) $B \approx 10 \div 15 (h^{-1} \text{Mpc})^{-D}$ ³².

The measured $n(r)$, the radial density computed only from *the origin*, therefore, scales as power law only beyond a certain scale. At smaller scales, the sampling fluctuations dominate the behaviour.

In LEDA, the scaling region begins at $\sim 15 h^{-1} \text{Mpc}$ and extends up to the limit of the sample, as shown in Fig.10.

The sample VL80 shows a fluctuation near the boundary, and has a $1/r^3$ decay up to $\sim 10 h^{-1} \text{Mpc}$ due to the depletion of points in this sample²¹.

Clearly, counting galaxies only from one observer induces larger statistical fluctuations than the $\Gamma(r)$ analysis, where one averages from *each point* of the sample.

7. POWER SPECTRUM

Similar results can be obtained by measuring directly the power spectrum, a statistics which is increasingly popular in cosmology. Let us recall the standard PS notation. If we have N galaxies in a survey volume V , we can expand the galaxy density contrast in its Fourier components: $\delta_{\vec{k}} = (\sum_j w_j)^{-1} \sum_{j \in V} w_j e^{i\vec{k}\vec{r}_j} - W(\vec{k})$, where w_j are statistical weights, and $W(\vec{k}) = V^{-1} \int d\vec{r} W(\vec{r}) e^{i\vec{k}\vec{r}}$ is the Fourier transform of the survey window $W(\vec{r})$, defined to be unity inside the survey region, and zero outside. To take into account the angular incompleteness $f(b, l) \in (0, 1)$ we take $w_j = 1/f(b, l)$. Of course, this corrects for the known angular incompleteness, leaving any residual radial gradient. We apply the standard power spectrum analysis, estimating the noise-subtracted PS for a strongly peaked window function as (see e.g. PVGH²²)

$$P(\vec{k}) = V_F \left(\langle |\delta_{\vec{k}}|^2 \rangle - \frac{\sum_j w_j^2}{(\sum_j w_j)^2} \right) \left(\sum_{\vec{k}} |W_{\vec{k}}|^2 \right)^{-1} (1 - |W_{\vec{k}}|^2)^{-1}. \quad (18)$$

The factor V_F , sometimes not explicitly written down because assumed conventionally to be unitary, is the arbitrary cubic volume, larger than the survey region, in which the window Fourier transform is evaluated. Notice that Fisher *et al.*²⁶ also investigate the PS of IRAS at several depths, but they take as sample density the density at fixed depth; this clearly renormalizes automatically the power spectrum amplitude, so that they would not detect any scaling even for a real fractal. The factor $(1 - |W_{\vec{k}}|^2)^{-1}$ has been introduced by Peacock & Nicholson²⁵ as an analytical correction to the erroneous identification of the sample density with the population density. For the lowest wavenumbers the power spectrum estimation (Eq.(18)) is not acceptable, because then the window filter flattens sensibly (see e.g. PVGH). The PS estimation is then accurate only up to the scale of the sample. This is shown in Fig.11, where to check our estimator we show the PS for two Poisson samples of 160 and 360 h^{-1} Mpc with the LEDA geometry and constant density: the numerical PS is accurate (i.e., constant and equal to the theoretical value V/N) only up to the survey scale.

In the homogeneous picture, the spectrum amplitude, just as the correlation function, is independent of the sample size R_s . The location of the flattening is also a real scale-independent feature. In the fractal picture, on the contrary, the PS scales as R_s^{3-D} , and a turnaround of the spectrum occurs systematically around R_s ³⁰. For instance, for $D = 2$ the analytical expression for the fractal PS in a sphere of radius R_s is $P(k) = (4\pi/3)[2 + \cos(kR_s)]R_s^{3-D}k^{-D} - 4\pi \sin(kR_s)k^{-3}$ ³⁰. The rapidly-varying functions of kR_s are in practice averaged out in the angular average of the spectrum.

The large number of galaxies present in the LEDA database allow us to disentangle the fractal scaling, which depends uniquely on the sample size, from the luminosity segregation, which depends on the average absolute magnitude of the galaxies in the sample. There is an almost general consensus, in fact, that intrinsically brighter galaxies cluster more than fainter ones; however, the strength of the effect, and the scale to which it extends are very uncertain issues^{46–50} The difficulty in reaching more extended and quantitative conclusions lies certainly in the relative scarcity of measured galaxy redshifts. For instance, the CfA2 survey contains only 608 galaxies (North plus South surveys) when

cut in a volume-limited sample at $130 h^{-1}\text{Mpc}$. With this small number, it is difficult to investigate the question of the dependence of the clustering amplitude with luminosity.

We begin with Leda14.5N, which is complete to about 90%, and consequently relatively free from strong selection effects. We plot in Fig.12 the PS for the samples as 40,80 and $100 h^{-1}\text{Mpc}$ (here we did not insert the Peacock-Nicholson correction factor, to show more clearly the turnaround scale). The spectra, as well as the turnaround scale, shift in agreement with the fractal prediction at all scales. This first result, which is already in conflict with the standard homogeneous view (unless one invokes a strong luminosity bias, see below), motivates us to go further.

We go then to Leda-CfA, which, as we already mentioned, has the same boundaries and the same magnitude limit as CfA2 .

We plot in Fig.13 the PS of the VL subsamples of Leda-CfA at 60, 101 and $130 h^{-1}\text{Mpc}$, respectively. As reported also in PVGH, the spectra amplitudes scale systematically with depth. The flattening, too, moves to larger and larger scales, as expected in the fractal view. Notice that if the scaling is caused by a *constant* bias factor, we should see a parallel scaling of the spectrum, rather than having the turnaround moving to larger scales. In the same figure we compare the spectra at 101 and $130 h^{-1}\text{Mpc}$ with the corresponding CfA spectra (PVGH). The agreement is reasonable, given that Leda is 70% complete at this depth. However, these volume-limited samples differ in average magnitude by increments of order $\Delta\hat{M} \approx 0.5$ so one may wonder if the luminosity biasing is responsible of the scaling. We calculated then the PS for all the fixed-depth, varying magnitude subsamples of Leda-CfA (Fig. 14).

As the figure shows, no clear sign of luminosity biasing can be detected. Notice also that the increments in magnitude range from $\Delta\hat{M} = 1.1$ within Leda-CfA60 subsamples to $\Delta\hat{M} = 0.3$ for Leda-CfA130. Only the most luminous galaxies, those with $\hat{M} = -20.8$ in Leda-CfA at $130 h^{-1}\text{Mpc}$, have higher amplitudes at scales $< 50h^{-1}\text{Mpc}$ than fainter samples. For as concern Leda-CfA, then, our conclusion is that the luminosity biasing does not explain neither the PS scale dependence, nor the constant scaling, nor the shift of the flattening scale. All three features, on the contrary, are naturally expected in a fractal clustering.

Finally we analyse Leda16N. We plot in Fig. 15 the PS of the three VL subsamples of Leda16N, at 60, 100 and 150 h^{-1} Mpc. The errors, here and in the following plots, are the scatter among several artificial fractal distributions with dimension $D = 2$, with the same geometry as the real surveys. In samples with N particles, the error bars have been rescaled as \sqrt{N} . The same scaling as in Leda-CfA is found up to the largest scale. The samples at 40 and 130 h^{-1} Mpc, not plotted in Fig. 15 for clarity, also follow the same scaling.

In Fig. 16 we report the PS of all the subsamples at fixed depths, and in Fig. 17 the PS in linear scale for the fixed-depth samples at 100 and 150 h^{-1} Mpc.

Here again, as for Leda-CfA, the trend with average magnitude is neither systematic, nor constant in scale. Only for as concerns samples brighter than $M = -20.5$ we notice a definite trend with luminosity. In Fig. 18, finally, we plot the PS at 60,100 and 150 h^{-1} Mpc averaged among all the subsamples at fixed depth. Overimposed, we plot the least squares fit and the fractal theoretical behavior with $D = 1.8$.

The agreement is clearly excellent. The fact that the scaling is k -independent is important also to reject the possibility that the scaling is induced by some kind of redshift distortion (see e.g. Fisher *et al.*1993); in fact, such an effect would depend strongly on wavelength. For a detailed discussion of the luminosity segregation in fractals we refer the reader to Sylos Labini and Pietronero (1996)⁶⁰. Multiplying the spectra of the Leda16N samples at $R_s = 60, 100, 130, 150h^{-1}$ Mpc samples by the factor $(150/R_s)^{3-D}$, with $D = 2$, we reconstruct (see Fig. 19) a single power spectrum (to be denoted as Leda-150), valid for a sample of depth $150h^{-1}$ Mpc, extending from a few Mpc to the sample size, in agreement with the fractal prediction.

If at larger scales the galaxies are homogeneous, our joint Leda-150 PS would represent our best estimate of the Universe PS; larger samples should then show no amplitude scaling and their PS should finally decrease to small values, possibly matching the COBE observations. The joint Leda-150 PS is well fitted by the scale invariant law k^{-D} , with $D \approx 1.8 \pm 0.1$. Then we may fit our Leda-150 PS with a standard CDM fit $P_{cdm} = AkT^2(k, \Gamma)$, where A and $\Gamma = \Omega h$ are free parameters, and $T(k, \Gamma)$ is the Davis *et al.*(1985)⁴⁴ transfer function. In the case of CfA2 the best fit parameters are around

$\Gamma \approx 0.23$ and $A \approx 10^6$. In the Leda-150 PS the fit with constant relative errors gives $\Gamma \approx 0.15$ and $A \approx 10^{7.3}$.

We performed two more tests on our PS. As already mentioned, Leda14.5 is almost complete, contrary to Leda16. However, the samples at $40 h^{-1}\text{Mpc}$ from Leda14.5N and Leda16N are consistent within the errors (see Fig. 20).

The same holds, although with a larger scatter, for the samples at $100 h^{-1}\text{Mpc}$. Further, we cut the Leda16N sample at $100 h^{-1}\text{Mpc}$ at various values of b . The spectra, plotted in Fig. 21 are all consistent with each other. If incompleteness seriously altered our results, we would have got strong random variations for the various b -cut catalogs, contrary to what we find. Notice also that smaller samples (higher b cut) have a smaller turnaround scale.

In summary, our conclusion based on the power spectrum analysis is that the fractal model accounts for the PS in the LEDA database up to $160 h^{-1}\text{Mpc}$. No sign of convergence to homogeneity is observed. Extending the analysis to $360 h^{-1}\text{Mpc}$ we find again an impressive agreement between the fractal prediction and the data, both for the North and the South samples, although we warn against incompleteness effects. If our conclusions are confirmed up to the largest scales, a major change in the interpretation of the galaxy clustering would probably be needed.

8. THE POWER SPECTRUM FIT

So far we did not pay close attention to the slope of the PS. We already noticed that all the PS shown in this paper have a behavior $\sim \lambda^D$ (i.e. $\sim k^{-D}$), with $D \approx 1.8$, as far as the sample finiteness does not distort the spectrum. We look now for the dependence of D with sample size and/or sample luminosity. We focus here on Leda16. Putting $P(k) = AR_s^{3-D}k^{-D}$ we report in Table III the full set of A, D for the Leda samples we analysed. The fit is performed for a sample at limiting depth R_s between the scales $.1R_s$ and R_s in order to avoid both the small scale aliasing and the large scale distortion. The ensemble average is $D = 1.67 \pm 0.17$ (although we prefer to quote the value of 1.8 because in closer agreement with results from Leda-CfA and other data). In Fig. 22 we report the slope D versus the average magnitude for all the Leda16 samples. A least square fit gives $D(M) = 0.008M + 1.5$,

indicating that there is no significant dependence of the fractal dimension on the absolute magnitude. In Fig. 23 we report the amplitude value $P_{50} = P(k = 2\pi/50h^{-1}\text{Mpc})$ and $P_{90} = P(2\pi/90h^{-1}\text{Mpc})$ versus R_s (bottom) and versus \hat{M} (top). While the dependence on R_s is clear, the dependence on \hat{M} is not systematic, except for the brightest samples, which indeed show a rise in power with magnitude, at $\hat{M} < -20.5$. In this range, the least square fit gives $\log(P) \sim -0.5M$.

9. COMPARISON WITH OTHER DATA

We can now compare our results for the space correlations analysis with those of other redshift surveys. In this respect, the first element that one has to consider is that the correlation function ($\Gamma(r)$ or $\xi(r)$) can be computed up to a limiting depth R_s . Given a certain catalog this depth is determined by the maximum depth *and the solid angle* (this is the reason why one needs to have surveys with large solid angles and not only deep pencil beams).

In particular the depth R_s is of the order of the radius of the maximum sphere fully contained in the sample volume¹⁹. This means for example that in the Las Campanas Redshift Survey⁵² ($R_{max} = 600h^{-1}\text{Mpc}$, $\Omega = 0.1sr$) $R_s \approx 20h^{-1}\text{Mpc}$. Such a value of R_s corresponds in terms of r_0 ($r_0 = (D/6)^{1/(3-D)}R_s$) to $\approx 6h^{-1}\text{Mpc}$ (if $D \approx 2$ as it has been measured in the LCRS), so that the value found is completely *compatible* with the fractal picture.

We consider now CfA2: in this case the published analysis of CfA2²² refers to a region with $R_{max} \approx 130h^{-1}\text{Mpc}$ and $\Omega \approx 1.2sr$ so that in this case $R_s \approx 35h^{-1}\text{Mpc}$ and hence $r_0 \approx 12h^{-1}\text{Mpc}$ as it results from the paper of Park and collaborators. Note that the linear scaling of r_0 with sample depth has been found also by these authors. Similar scalings have been obtained in SSRS2⁵⁰ and the Optical redshift Survey (ORS)⁵³. In the first case, the scaling has been attributed to luminosity segregation. This conclusion, however, is based on very sparse sampling (particularly on a volume-limited sample at $91 h^{-1}\text{Mpc}$ which contains only 67 galaxies) and, moreover, directly contradicts the fact that in CfA2, in Las Campanas⁵² and in the same SSRS2⁹, the luminosity biasing was found to be insufficient. In ORS⁵³, the luminosity segregation is explicitly rejected, and the scaling from 40 to $80 h^{-1}\text{Mpc}$ is attributed generically to large scale inhomogeneities. Consider now another

catalog: Perseus-Pisces. In this case in Sylos Labini *et al.*²⁰ (see also Guzzo *et al.*²⁸) it was found that $R_s \approx 30h^{-1}\text{Mpc}$ and $r_0 \approx 11h^{-1}\text{Mpc}$, and a very well defined linear scaling of r_0 with sample depth (this result is implicit in the Guzzo *et al.*²⁸: as far as $\Gamma(r)$ has a power law behaviour, as Guzzo *et al.*²⁸ found up to $\sim 30h^{-1}\text{Mpc}$, r_0 *must* be a linear function of the sample size, independently from the fact that the distribution would eventually become homogenous at much larger distances). Finally in CfA1¹⁹ a linear scaling of r_0 has been found up to the value $r_0 \approx 6 - 7h^{-1}\text{Mpc}$ for $R_s \approx 20h^{-1}\text{Mpc}$.

However there are still some points that seems to be compatible with homogeneity: the IRAS redshift surveys and the behaviour of angular correlation function as a function of sample depth. Both these evidences are, in our opinion, an artifact due to finite size effects. We now discuss briefly these points, but we refer to Sylos Labini *et al.*³² for a more detailed discussion.

Let us start with the IRAS surveys. Suppose we have a finite portion of a real fractal, and that we select randomly only a fraction of the points belonging to the fractal set. It is clear that if the number of points is very small, the underlying fractal properties cannot be recovered. Rather, the set of points will look as a very sparse uncorrelated structure. The point we are going to make in a forthcoming publication is that this sparse fractal set *will look like a (noisy) homogeneous sample*. We can prove this statement by analytical and numerical techniques. Let us compare the samples we are considering. The CfA1 sample has about 1000 galaxies per steradian, the Perseus-Pisces (PP) 3000/sr, IRAS 2Jy 200/sr and IRAS1.2 Jy 400/sr (we are comparing galaxies per steradian since the average depth of these samples is not very different). For CfA2 this number is much larger than that of PP. As one can see, the IRAS samples are by far the most sparse sample: this is the reason, in our view, why they do not show the expected correlation scaling. In other words, the different results of the IRAS samples with respect to that of the optical catalogues (CfA1, CfA2, Las Campanas, SSRS2, ORS, and Perseus Pisces) can be attributed to systematic effects due to the poor sampling. Notice that this explanation holds irrespective of the fractal viewpoint: the IRAS and optical data are different, and no clear explanation has been offered to date. Consider also that the visual impression confirms that the IRAS galaxies do *not* fill the optical voids; rather, they belong to the same structure of the optical galaxies. Hence it is very puzzling how the large voids of tens of megaparsecs seen both in optical and

infrared surveys can be compatible with a very small correlation length ($4h^{-1}\text{Mpc}^{54,55}$). Our results show very clearly that the two IRAS samples are not statistically fair samples because they contain too few points per unit volume. We added some comments on this in the conclusions.

The problem of the angular correlation function is very close to the problem of the IRAS data. In the IRAS data the problem is that the survey is too sparse to see fractality; in angular data the problem is that we are seeing only one single sky, and thus, even if there is a large number of points in the survey, we cannot make an average over observers (the *angular* average that is performed in angular correlation function does not help, because it does not include depth). We prove in a forthcoming paper that the angular correlation function of a fractal as populated as the real APM survey gives the same “homogeneous” scaling observed in that survey. Were we able to perform an average over observers, the ”scaling” would disappear, as expected in a fractal. Exactly the same argument applies, of course, to the number counts. The argument of Peebles³¹ on the angular correlation function of a fractal is correct, but incomplete, not taking into account the statistical significance of real surveys. Note in this respect that one should also explain the contradiction between the scaling (linear or not) observed in optical redshift survey, and the scaling observed in angular correlation functions: the latter in fact is not compatible with the former, as is clear from the Limber equation. On the contrary, they are fully compatible within our view.

10. DISCUSSION AND CONCLUSIONS

In this paper we have discussed the statistical properties of galaxy distribution in the LEDA database. This is the largest galaxy redshift catalog currently available. We have shown that, although this sample is seriously affected by incompleteness, the statistical global properties of the galaxy distribution are quite stable. We stress once again that we are detecting a *correlated signal*: if this were due to the effects of ”inhomogeneous holes” in the selection procedure, then these artificial features should have very peculiar properties, i.e. they should be fractal with the same dimension detected in the regions where the incompleteness is lower or absent. This means that they must be scale invariant in a well defined way. But this seems rather peculiar. In fact, while it is easy, performing

a random sampling of a structure characterized by long-range correlations (i.e. a fractal), to destroy the correlations because of incompleteness effects, it seems very difficult, on the contrary, to create them.

The result is that the galaxy distribution has a well defined fractal behaviour with $D \approx 2$ up to $\sim 200h^{-1}\text{Mpc}$, that is the limit of statistical validity of this sample. No tendency towards homogenization has been detected at deeper distances. We have discussed in detail the compatibility of these results with those found in different and more complete samples of galaxies by different authors. The main problem of all these analyses is that they are based on the assumption that the large scale galaxy distribution is homogeneous. In this paper we have tested this fundamental assumption, finding that galaxy distribution exhibits a highly irregular nature characterized by self-similarity. The regime of fractal behaviour is found to extend to more than three decades in the density. These results can be confirmed or confuted by the forthcoming survey like the Sloan Digital Sky Survey.

REFERENCES

1. Davis, M., in the Proc of the Conference "Critical Dialogues in Cosmology" N. Turok Ed. (1997) World Scientific
2. Pietronero L., Montuori M., Sylos Labini F., in the Proc of the Conference "Critical Dialogues in Cosmology" N. Turok Ed. (1997) World Scientific
3. Kirshner R.P., Oemler A., Schechter P.L., Shectman S.A., 1981, ApJ Lett. 248, L57
4. Einasto J., Corwin H.G., Huchra J., Miller R.H., Tarenghi, 1983, *Highlights of Astronomy*, Vol. 6, ed. R. West, Reidel, Dordrecht, p. 757
5. Huchra, J., Davis, M., Latham, D., Tonry, J. *Astrophys. J. Suppl.*, 52, (1983) 89.
6. De Lapparent, V., Geller, M. J., Huchra, J. P. *Astrophys. J.* 332, (1988) 44
7. Broadhurst, T. J., *et al.* *Nature*, 343, (1990) 726
8. Vettolani, G., *et al.* (1994) Proc. of Schloss Rindberg workshop Studying
9. Da Costa, L. N. *et al.* *Ap. J.* 424, (1994) L1
10. Paturel, G., Bottinelli, L., Gouguenheim, L., *Astron. Astrophys.* 1994, 286, 768
11. Paturel, G., Bottinelli, L., Di Nella, H., Durand, N., Garnier, R., Gouguenheim, L., Lanoix, P., Marthinet, M.C., Petit, C., Rousseau, J., Theureau, G., Vauglin, I., *Astron. Astrophys.* 1996, in press
12. Paturel g., Vauglin I., Garnier R., Marthinet M.C., Petit C., Di Nella H., Bottinelli L., Gouguenheim L., Durand N., in "Databases and On-Line data in astronomy" Eds. Egert D. and Albrecht M., (1995) Kluwer Academic Publisher
13. Paturel, G., Bottinelli, L., Gouguenheim, L., Fouque, P. *Astron. Astrophys.*, 189, (1988) 1
14. Di Nella H., and Paturel G., *Comptes rendus de l'Academie des Sciences Paris, serie II*, t319, (1994) 57
15. Davis, M., Peebles, P. J. E. *Astrophys. J.*, 267, (1983) 465

16. Peebles, P.J.E. Large Scale Structure of the Universe , Princeton Univ. Press
17. Pietronero L., Physica A, 144, (1987) 257
18. Coleman, P.H. Pietronero, L.,& Sanders,R.H., Astron. Astrophys. Lett. 245, (1988), 1
19. Coleman, P.H. & Pietronero, L., Phys.Rep. 231, (1992) 311
20. Sylos Labini F., Montuori M., Pietronero L., Physica A, (1996) 230, 336
21. Sylos Labini F., Montuori M., Pietronero L., (1997) preprint
22. Park, C., Vogeley, M.S., Geller, M., Huchra, J. Astrophys. J., 431, (1994) 569
23. Da Costa *et al.*, (1994) Ap.J. 437,L1 .
24. Baugh C.M. and Efstathiou G. Mon.Not.R.Acad.Soc, 267 (1994) 323
25. Peacock, J.A., Nicholson, D. Mon.Not.R.Acad.Soc 235, (1991) 307 au
26. Fisher et al. 1993, Astrophys.J., 402, (1993) 42
27. Feldman H. A., Kaiser, N., & Peacock, J.A. 1994, Ap. J., 426, 23
28. Guzzo L., *et al* Astrophys. J., 382, (1992) L5
29. Maddox *et al.*, Mon.Not.Royal Ac. Soc 242, (1990) 43
30. Sylos Labini, F. Amendola, L. Ap.J., 468, (1996) L1
31. Peebles P. J. E., (1993) Principles of physical cosmology, Princeton Univ. Press
32. Sylos Labini F., Gabrielli A., Montuori M., Pietronero L., Physica A, 226, (1996) 195
33. de Vaucouleurs G., 1953, Astron. J 58, 30
34. de Vaucouleurs G., 1956, Vistas Astr. 2, 1584
35. Geller M. and Huchra J., 1988, Science 246, 897
36. Zeldovich Y.B., 1970, A&A 5, 84
37. Da Costa, L. N. *et al.* Ap. J., 327, (1988) 544
38. Fairall A.P., Palumbo G.G.C., Vettolani G., Kauffmann G., Jones A., Baiesi-Pillastrini G., 1990, MNRAS 247, 21

39. Gregory S.A., Thompson L.A., Tifft W., 1981, ApJ 243, 411
40. Haynes, M., Giovanelli, R., (1988) in "Large-scale motion in the Universe", Eds. Rubin, V.C., Coyne, G., Princeton University Press, Princeton
41. Bottinelli L., Gouguenheim L., Fouqué P., Paturel G., 1986, in *La Dynamique des Structures Gravitationnelles*, Observatoire de Ly on
42. Mandelbrot B., (1982) *The Fractal Geometry of Nature*, Freeman, New York
43. Schechter, P., *Astrophys.J.* 203, (1976) 297
44. Davis M. *et al.*1985, *Ap. J.*, 292, 371
45. Bennett C.L. *et al.**Ap.J.*, 436 (1994), 423
46. Hasegawa *et al.*1993 *MNRAS*, 263, 191
47. Martinez V. J. 1993, *A& A*, 280, 5
48. Dominguez-Tenreiro R. *et al.*1994, *Ap. J.*424, L73
49. Loveday J.*et al.*1995 *Ap. J.*, 442, 457
50. Benoist C., Maurogordato S., Da Costa L.N., Cappi A., and Schaeffer R., *Ap. J.*, (1996), in print
51. Dogterom M. and Pietronero L., *Physica A* (1991) 171, 239
52. Tucker D.L. *et al.*, *MNRAS* (1996) in press, (astro-ph/9611206)
53. Hermit S.*et al.*, *MNRAS*, 283, 709
54. Strauss M.A., *et al.*, *Astrophys.J.Suppl.* 83, (1992) 29
55. Fisher K., *et al* *Mon.Not.R.Acad.Soc* 266, (1994) 50
56. Landy et al. 1996, *Ap. J.*, 456, L1
57. Erzan A., Pietronero L., Vespignani A., *Rev. Mod. Phys.* 67, (1995) 554
58. Baryshev, Y., Sylos Labini, F., Montuori, M., Pietronero, L. *Vistas in Astron.* 1994, 38, 419
59. Pietronero L. & Tosatti E., Eds (1986) *Fractal in Physics* North-Holland, Amsterdam
60. Sylos Labini F. & Pietronero L., *Astrophys.J.*, 469 (1996), in print

TABLES

TABLE I. The VL subsamples of LEDA14.5N-CfA1 ($\Omega = 1.8$)

SAMPLE	$d_{lim}(h^{-1}Mpc)$	M_{lim}	N	p
VL40	40	-18.54	445	8 %
VL60	60	-19.43	320	2 %
VL80	80	-20.07	226	1.1 %

TABLE II. The VL subsamples of LEDA14.5N and LEDA14.5S (North N=4703, South N=4163) (cut in absolute magnitude)

Sample	$d_{lim}(h^{-1}Mpc)$	M_{lim}	N
VL18S	31.3	-18.00	578
VL18N	31.3	-18.00	1138
VL185S	39.3	-18.50	712
VL185N	39.3	-18.50	1120
VL19S	49.3	-19.00	1034
VL19N	49.3	-19.00	1095
VL195S	61.8	-19.50	1160
VL195N	61.8	-19.50	844
VL20S	77.4	-20.00	675
VL20N	77.4	-20.00	634
VL205S	96.9	-20.50	371
VL205N	96.9	-20.50	282

TABLE III. The VL subsamples of LEDA16N and LEDA16S (North N=13362, South N=11794) (cut in absolute magnitude)

Sample	$d_{lim}(h^{-1}Mpc)$	M_{lim}	N
VL18S	61.8	-18.00	4402
VL18N	61.8	-18.00	4011
VL185S	77.4	-18.50	4632
VL185N	77.4	-18.50	4827
VL19S	96.9	-19.00	4481
VL19N	96.9	-19.00	4678
VL195S	121.0	-19.50	3724
VL195N	121.0	-19.50	3761
VL20S	150.9	-20.00	2463
VL20N	150.9	-20.00	2143
VL205S	187.8	-20.50	1305
VL205N	187.8	-20.50	905

$d(Mpc) :$	20	40	60	80	100	120	140	160	180	200
$N_{gal} :$	1037	2774	3945	4939	5310	5507	5593	5643	5661	5683
$lp(deg) :$	46	46	46	51	52	52	52	52	52	52
$bp(deg) :$	14	14	17	16	16	16	16	16	16	16
$\%gal :$	55	46	46	45	45	44	44	44	44	44

TABLE IV. N_{gal} is the number of galaxies located at a distance shorter than d and $\%gal$ is the percentage of galaxies located within ± 15 deg of the plane defined by the pole of coordinates lp et bp . This corresponds to the most populated plane within the volume of Universe of radius d . This percentage is much larger than what expected for an homogeneous distribution of galaxies

VL $d(Mpc)$	Angular coverage	Btlim	Mlim	number of galaxies	lpole	bpole	% of galaxies
20	all sky	14.5	-17.0	1167	45	14	57
20	all sky	16	-15.5	2145	43	14	49
80	all sky	14.5	-20.0	1112	57	21	47
80	1/2 sky	14.5	-20.0	555	60	18	47
80	all sky	16	-18.5	8506	59	12	44
80	1/2 sky	16	-18.5	3934	58	18	44
150	all sky	16	-19.9	4476	59	3	39
150	1/2 sky	16	-19.9	2275	59	3	43

TABLE V. Summary table for the research of a privileged plane within different Volume Limited samples.

The pole of the Local Supercluster ($d < 20$ Mpc) is found close to the published value by De Vaucouleurs in the RC2 ($l=47\text{deg}$, $b=6\text{deg}$) with 57% of galaxies of the sample located in the region of ± 15 deg of the plane. On large scale the hypergalactic plane is present with roughly 40% of the galaxies in the region of ± 15 deg of the plane.

FIGURES

FIG. 1. To investigate the completeness of the database in terms of rate of measurements in a survey, we plot the number of galaxies with a known magnitude (dashed line) and the number of these galaxies having a measured redshift in LEDA (continue line). This plot shows the completeness for LEDA at $B_T < 17$ (half-sky). Up to $B_T \sim 14.5$, 90% of the known galaxies are measured in redshift. After this limit, the database begins to be incomplete.

FIG. 2. Flamsteed's equal area projection in supergalactic coordinates showing a structure connecting Perseus-Pisces, Pavos-Indus and Centaurus Supercluster (see Paturel et al, 1988)

FIG. 3. Face-on view of the hypergalactic plane, slice of 100 Mpc on the Z axis. Each point corresponds to a galaxy. Ours is located at the origins of the coordinates. We can see that our position is in the outskirts of the Local Supercluster, which is itself centered on the Virgo cluster. Some observational artifacts are clearly seen: the zones without redshift measurements due to the absorption of the Milky Way (vertical trace) and the radial elongation of the galaxy clusters (in particular in periphery). The local Supercluster seems surrounded by an empty region, delimited by the neighbor superclusters : Centaurus, Pavo-Indus, Perseus-Pisces and the Great Wall.

FIG. 4. Perpendicular view to the hypergalactic plane. Slice of 100 Mpc on the X axis. On this view the Great Wall is clearly curved in direction of the Local Supercluster. One can also see clusters of galaxies elongated radially (see the text for explanation). The major part of the galaxies are localized between +50 Mpc and -50 Mpc on the Z axis, which correspond to the hypergalactic plane seen by the side.

FIG. 5. The conditional average density $\Gamma^*(r)$ for various VL samples of the LEDA14.5 sample. N for the VL sample of the Northern hemisphere and S for the Southern one. The reference line has a slope $-\gamma = -0.9$ ($D = 2.1$).

FIG. 6. The conditional average density $\Gamma^*(r)$ for various VL samples of the LEDA16 sample. N for the VL sample of the Northern hemisphere and S for the Southern one. The reference line has a slope $-\gamma = -0.9$.

FIG. 7. The conditional average density $\Gamma^*(r)$ for the VL sample 2N280 LEDA16 sample. The filled circles refer to the $\Gamma(r)$ of the total sample, the squares for the first half (0-160 h^{-1} Mpc) and the diamonds for the second half (160-360 h^{-1} Mpc).

FIG. 8. The spatial density $\Gamma^*(r)$ computed in some VL samples LEDA and normalized to the corresponding luminosity factor.

FIG. 9. Behaviour of the so-called "correlation length" as a function of the sample size. The reference line has a linear behaviour is in agreement with the fractal prediction. It is remarkable to note that in the deepest sample we find $r_0 \approx 45 \pm 5h^{-1}$ Mpc.

FIG. 10. The spatial density $n(r)$ computed in some VL samples of LEDA145. A very well defined power law behavior with $D \approx 2$ is shown for $r \gtrsim 15h^{-1}$ Mpc $\approx \lambda$.

FIG. 11. Top panel: the PS of two artificial Poisson samples of depth 160 (circles) and 360 (squares) h^{-1} Mpc, with the Leda window geometry. Bottom panel: the window PS of the two samples.

FIG. 12. The PS (without Peacock-Nicholson correction) of the three VL samples of Leda14.5N at 40, 80, and 100 h^{-1} Mpc, from bottom to top, respectively. The lines are best fit to the data (at scales smaller than the turnaround). The systematic shift in the amplitude, and in the location of the flattening is clear.

FIG. 13. The PS of the VL samples of Leda-CfA at 60, 100, and 130 h^{-1} Mpc, from bottom to top, respectively. The thin line indicates a slope of $D = 2$. The systematic shift in the amplitude, and in the location of the flattening is clear. Also shown are the data from CfA2-101 and CfA2-130 PS (from PVGH).

FIG. 14. Leda-CfA PS at various average magnitudes. No clear luminosity trend can be detected.

FIG. 15. The PS of the VL samples of Leda16 at 60, 100 and 150 h^{-1} Mpc, from bottom to top, respectively. The top thin line indicates a slope of $D = 2$, the dotted lines are the best fits to the data. For sake of clarity we plot the errorbars only on two sets of data. The systematic shift in the amplitude is clear.

FIG. 16. Leda16 PS at various average magnitudes.

FIG. 17. Leda16 relative amplitudes for various subsamples in linear scale. Top panel: samples at $100 h^{-1}\text{Mpc}$; bottom panel: samples at $150 h^{-1}\text{Mpc}$. The brightest samples show some luminosity dependence.

FIG. 18. Average PS of the equal-depth subsamples of Leda16 at 60, 100 and $150 h^{-1}\text{Mpc}$. The dotted lines are the least square fits; the solid lines are the fractal predictions with $D = 1.8$.

FIG. 19. The PS of the average samples at 60, 100, 130 and $150 h^{-1}\text{Mpc}$ of Leda16 rescaled according to the fractal model with $D = 1.8$ to a depth of $150 h^{-1}\text{Mpc}$. The curve is a CDM-like fit with $\Gamma = 0.15$.

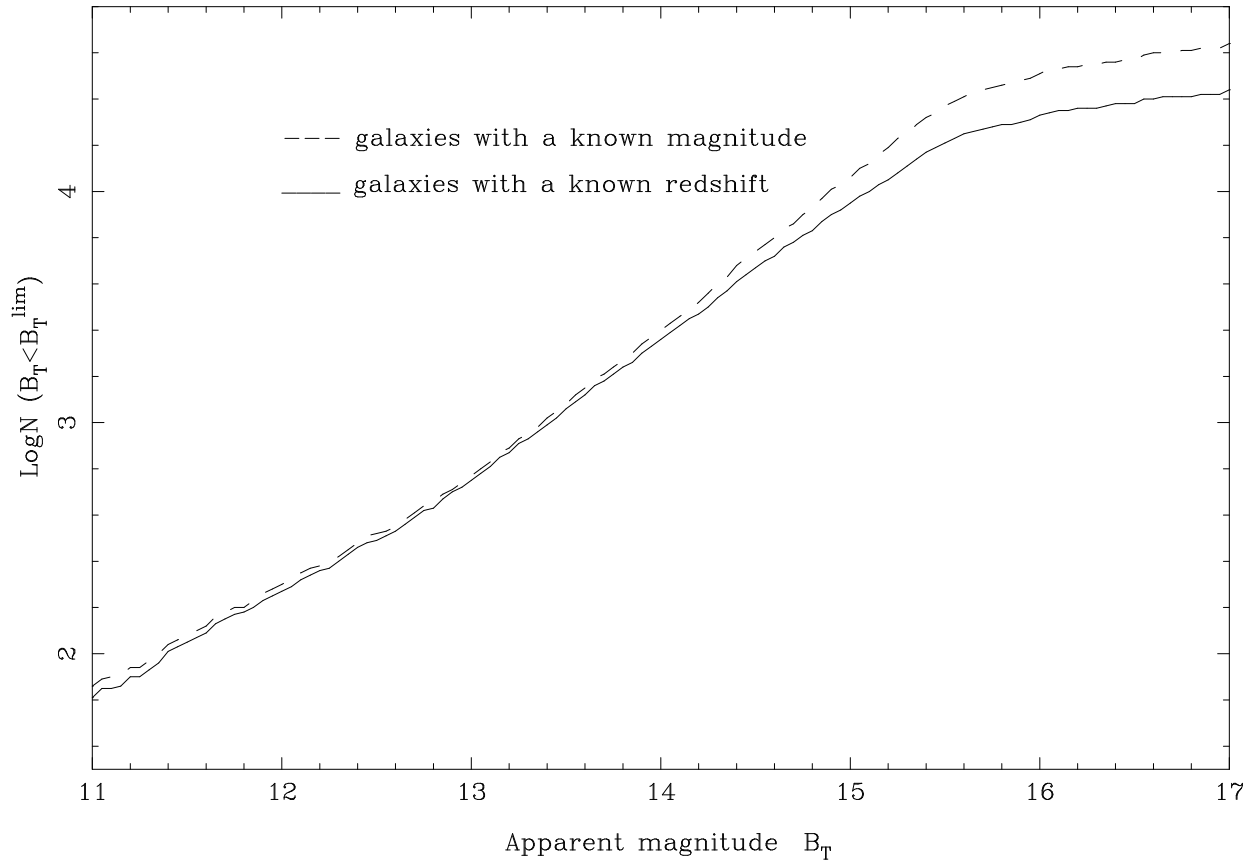
FIG. 20. Comparison of spectra at scales of 40 and $100 h^{-1}\text{Mpc}$ for samples from Leda14.5 and Leda16 , which have very different levels of incompleteness. The spectra are consistent within the typical scatter. The solid lines are the best fits to the 14.5 samples.

FIG. 21. The PS of the $100 h^{-1}\text{Mpc}$ VL Leda16N samples cut at $b > 20^0, 30^0, 40^0, 50^0$ and 60^0 .

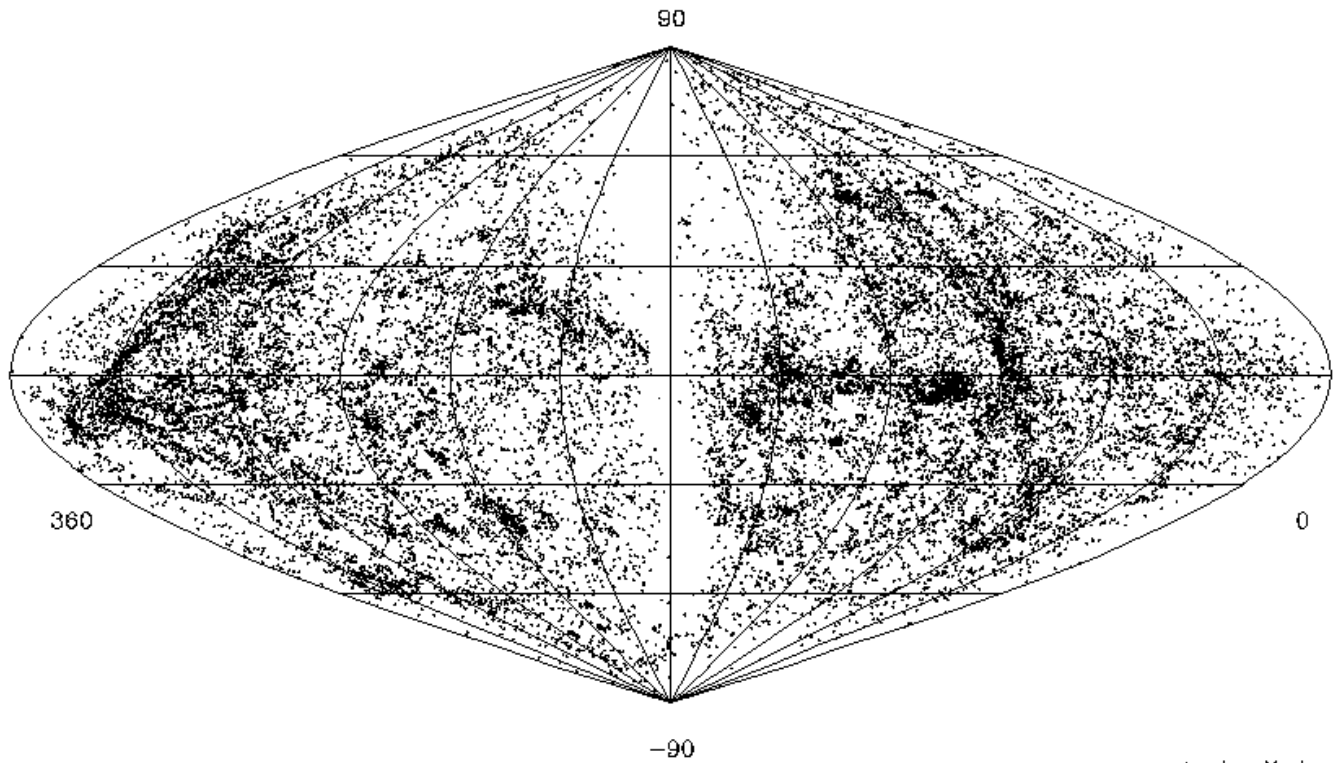
FIG. 22. Fractal dimension versus average absolute magnitude. The continuous line is the ensemble average dimension, $D = 1.67$; the two dotted lines give the root-mean-square errors.

FIG. 23. The amplitudes P_{50}, P_{90} versus sample depth (bottom) and sample average magnitude (top). In the bottom panel, squares report P_{50} , circles report P_{90} , and the dotted line is the fractal scaling trend for $D = 1.8$. In the top panel, open squares, open circles, and filled squares represent P_{50} for samples at 60, 100 and $150 h^{-1}\text{Mpc}$, respectively; open triangles, crosses and filled triangles give P_{90} for the same samples. Only the brighter samples show a definite monotonous increase of power with luminosity.


Completeness curve for LEDA17 (half-sky)

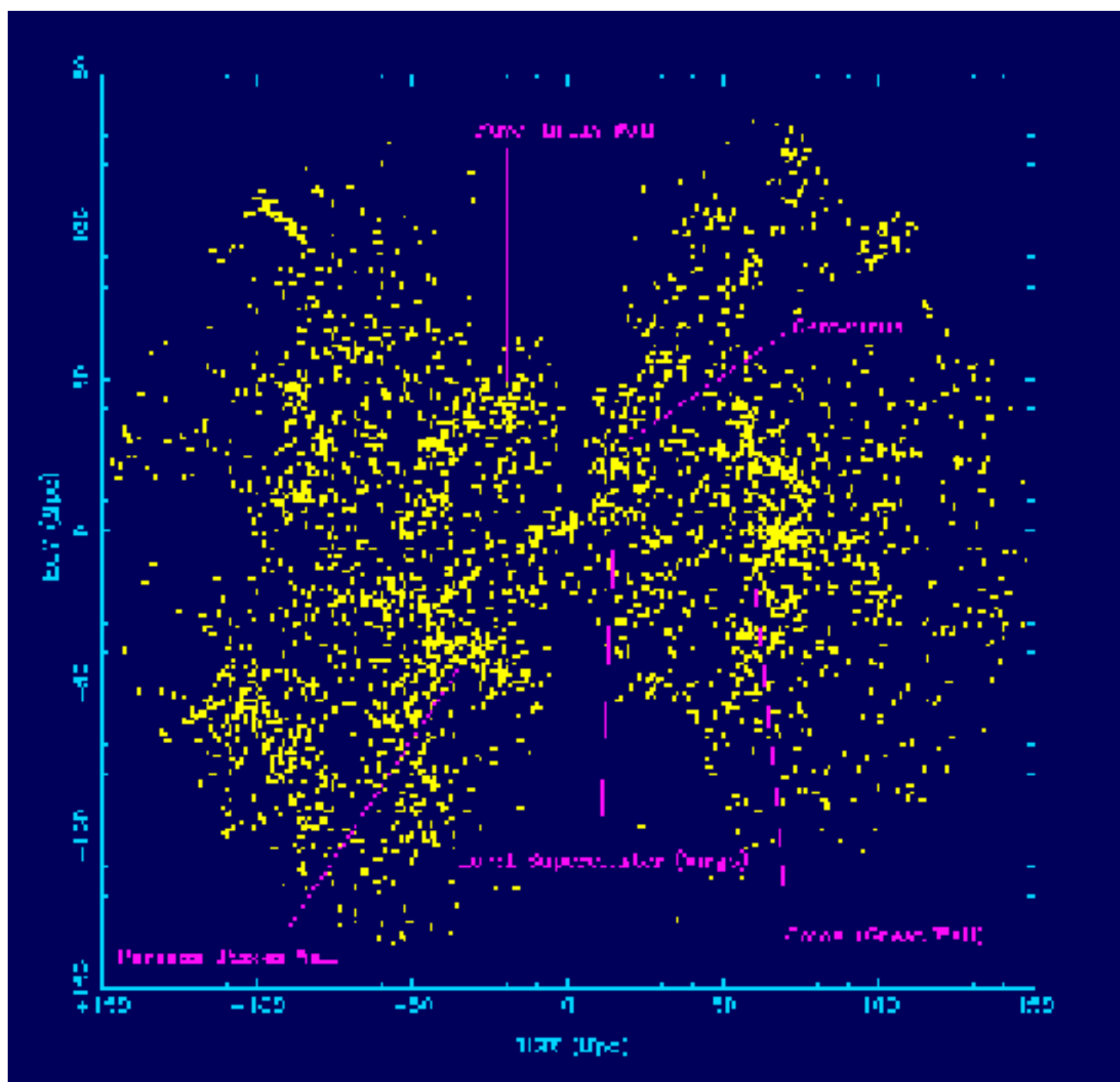


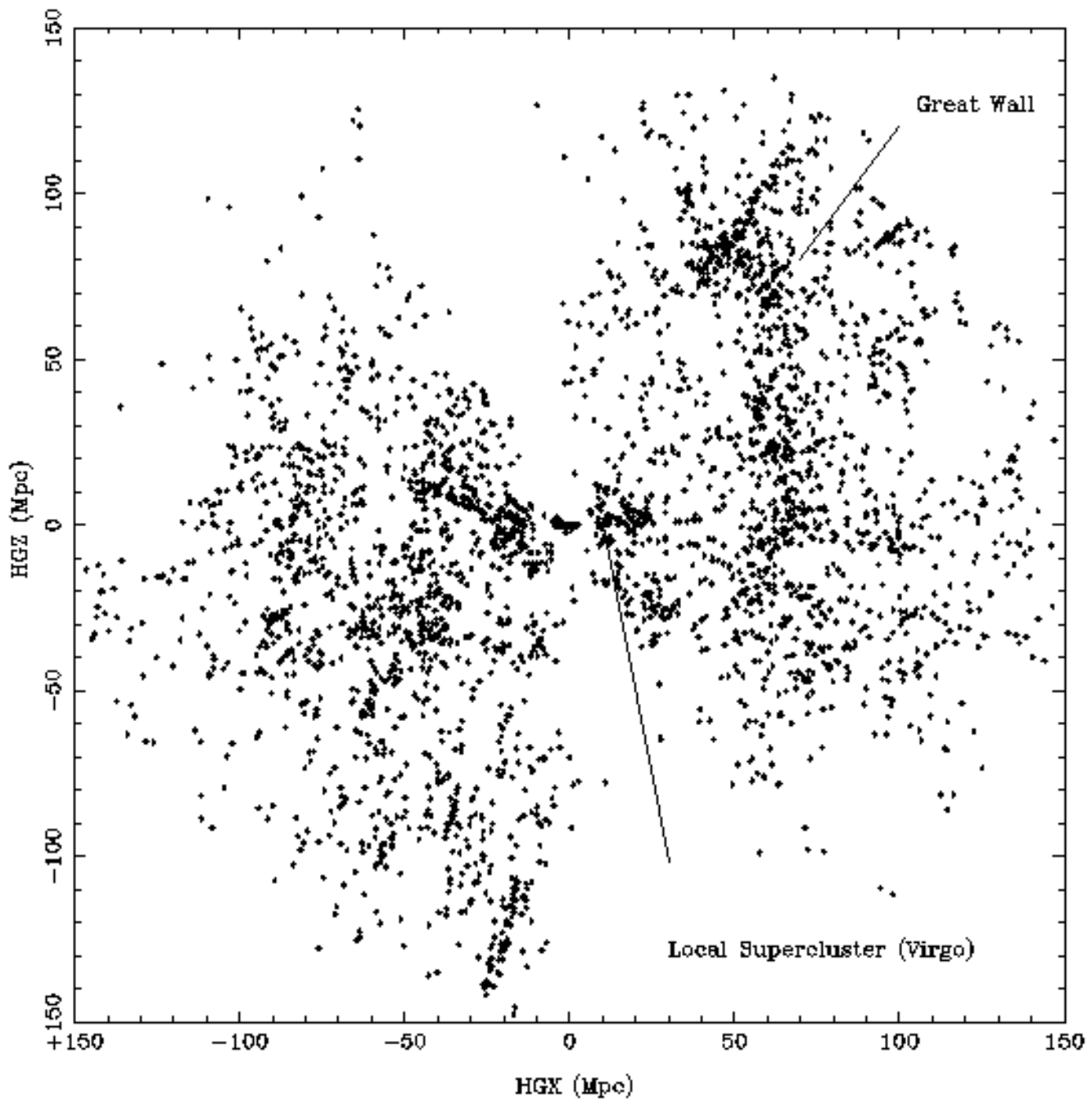
Flamsteed equal area projection for 27045 galaxies in supergalactic coordinates

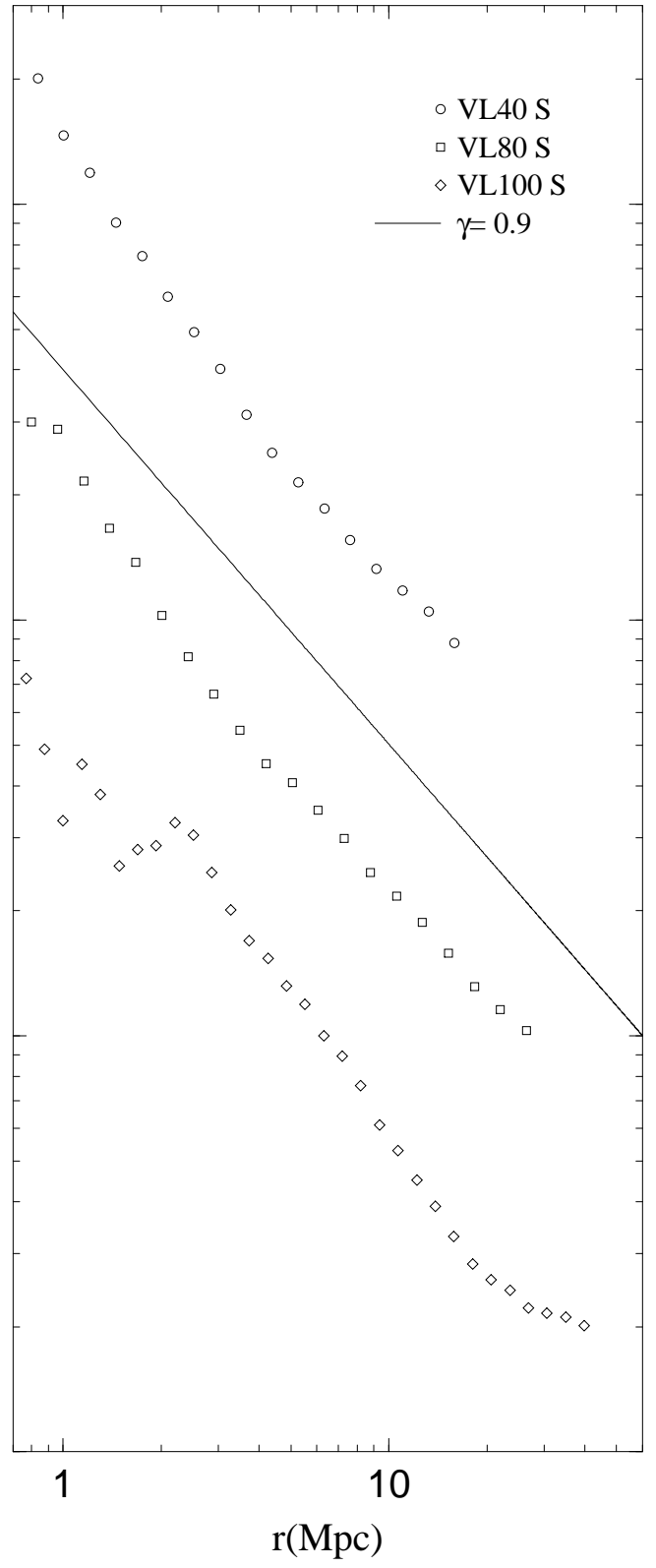
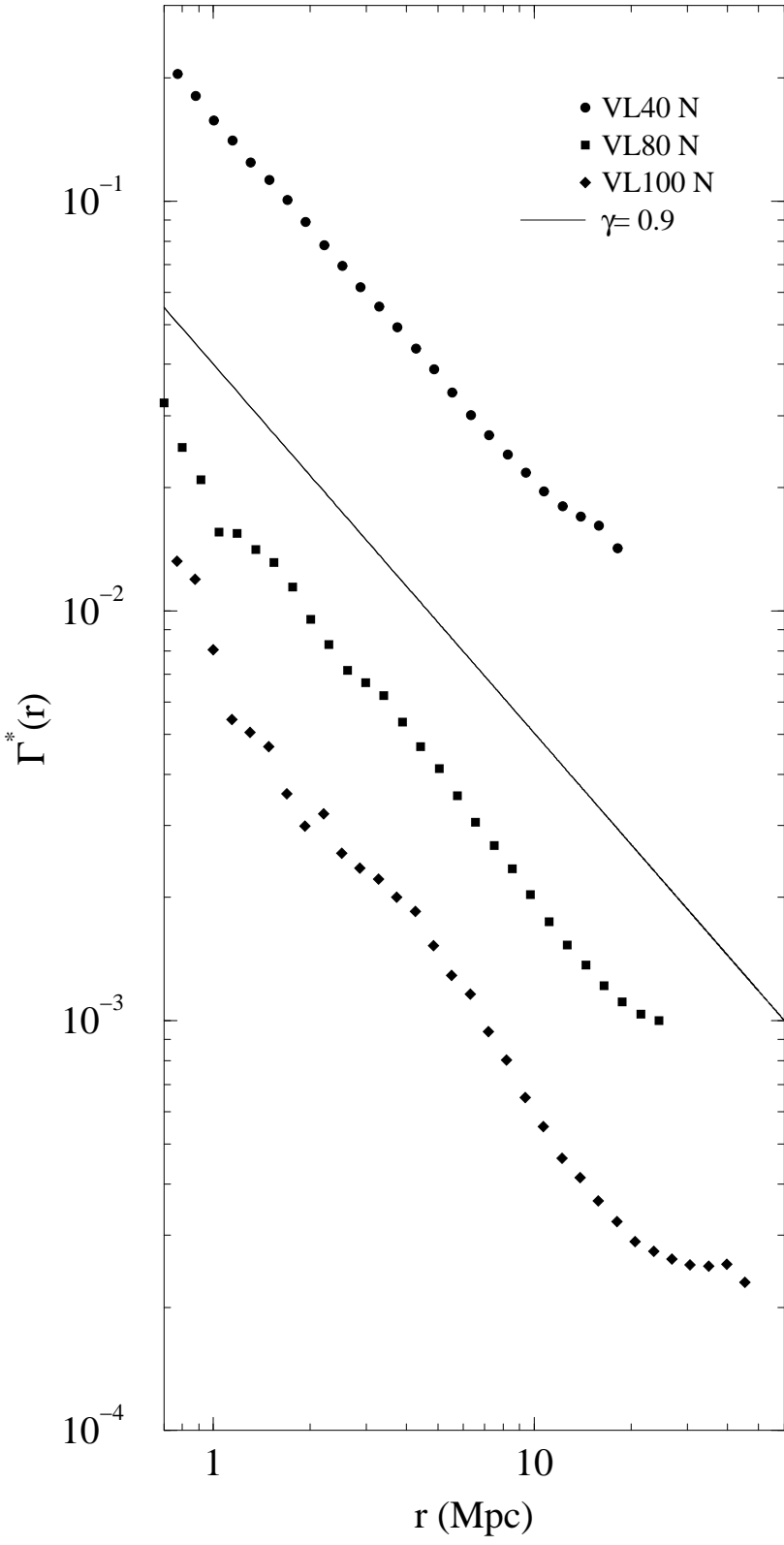


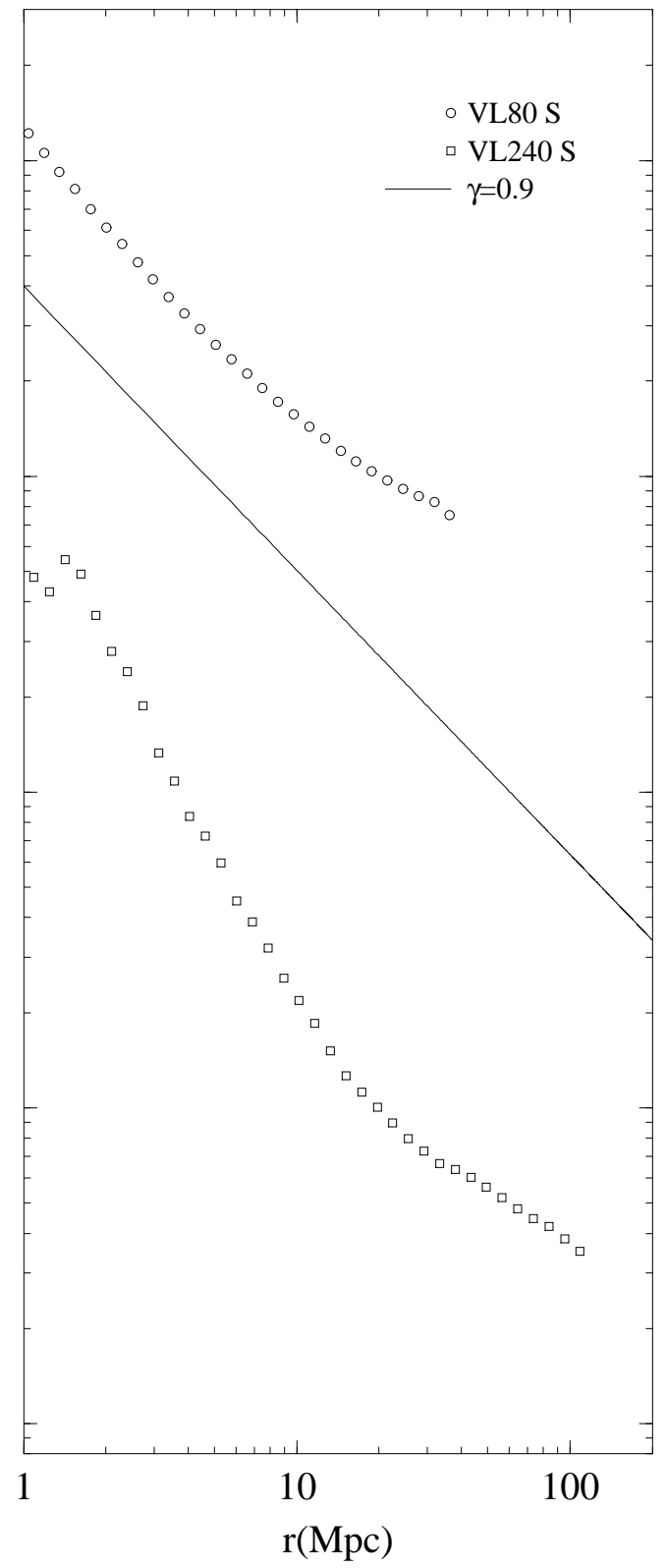
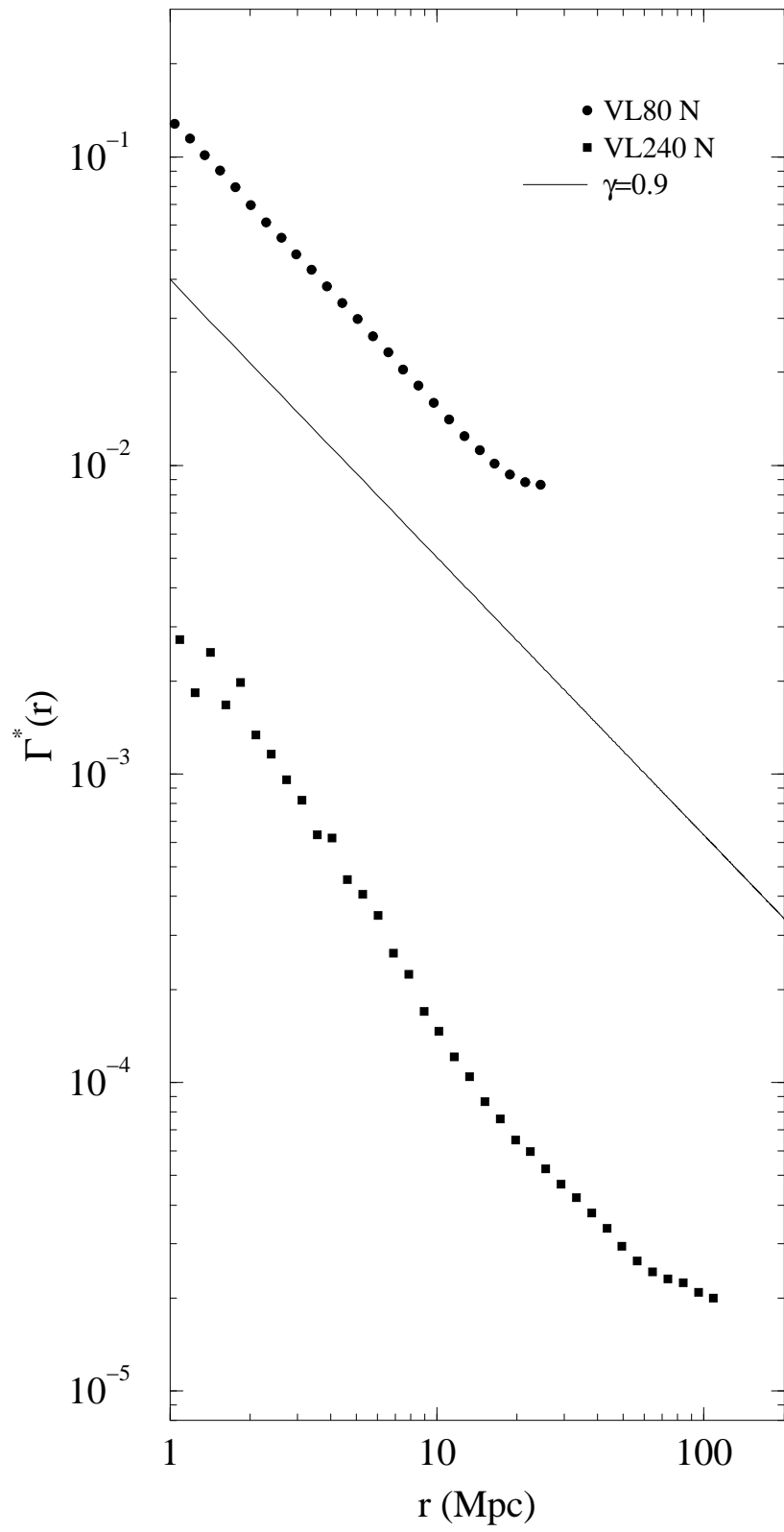
LYON MEUDON EXTRAGALACTIC DATABASE

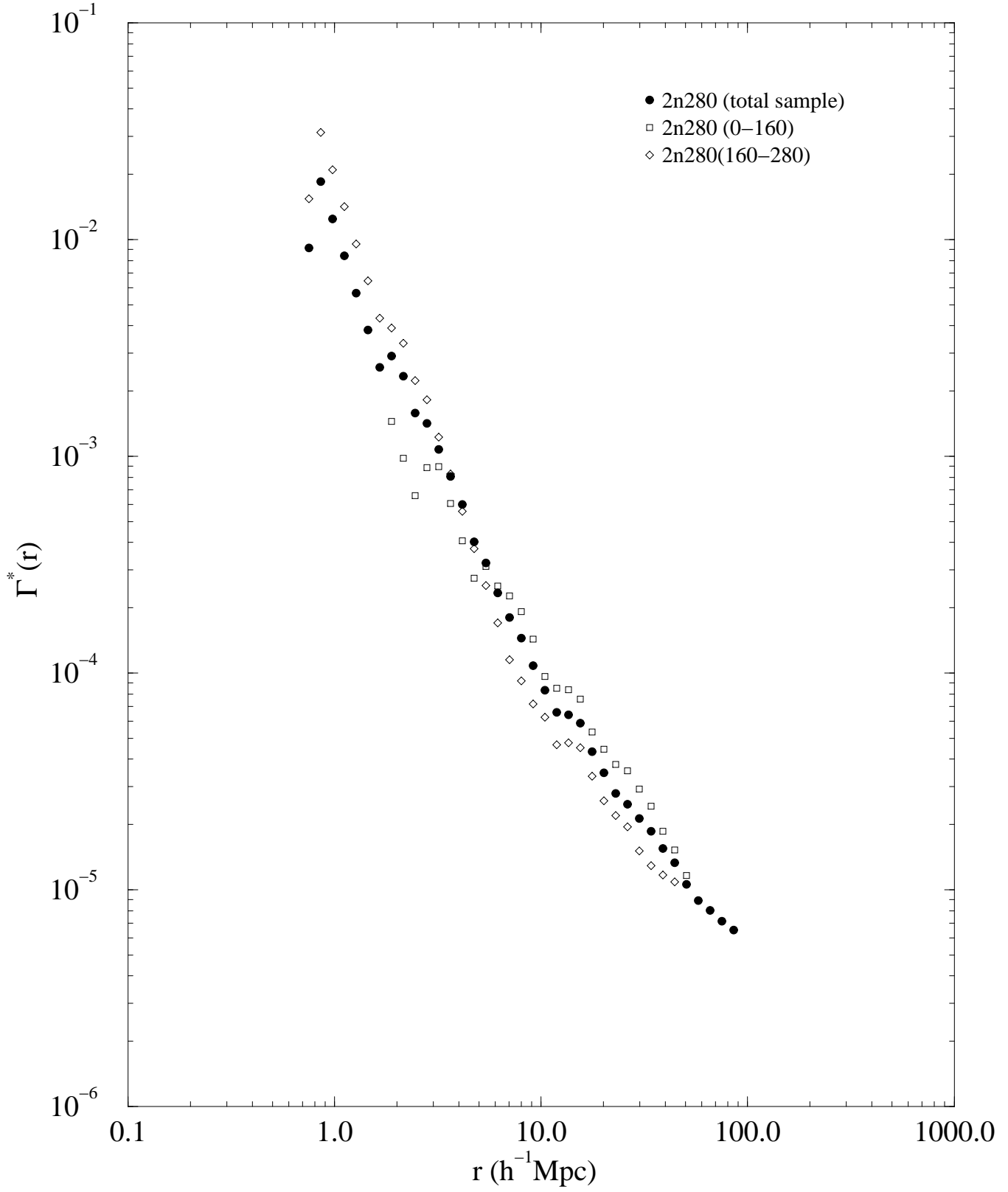
 Lyon Meudon
Extragalactic
Database

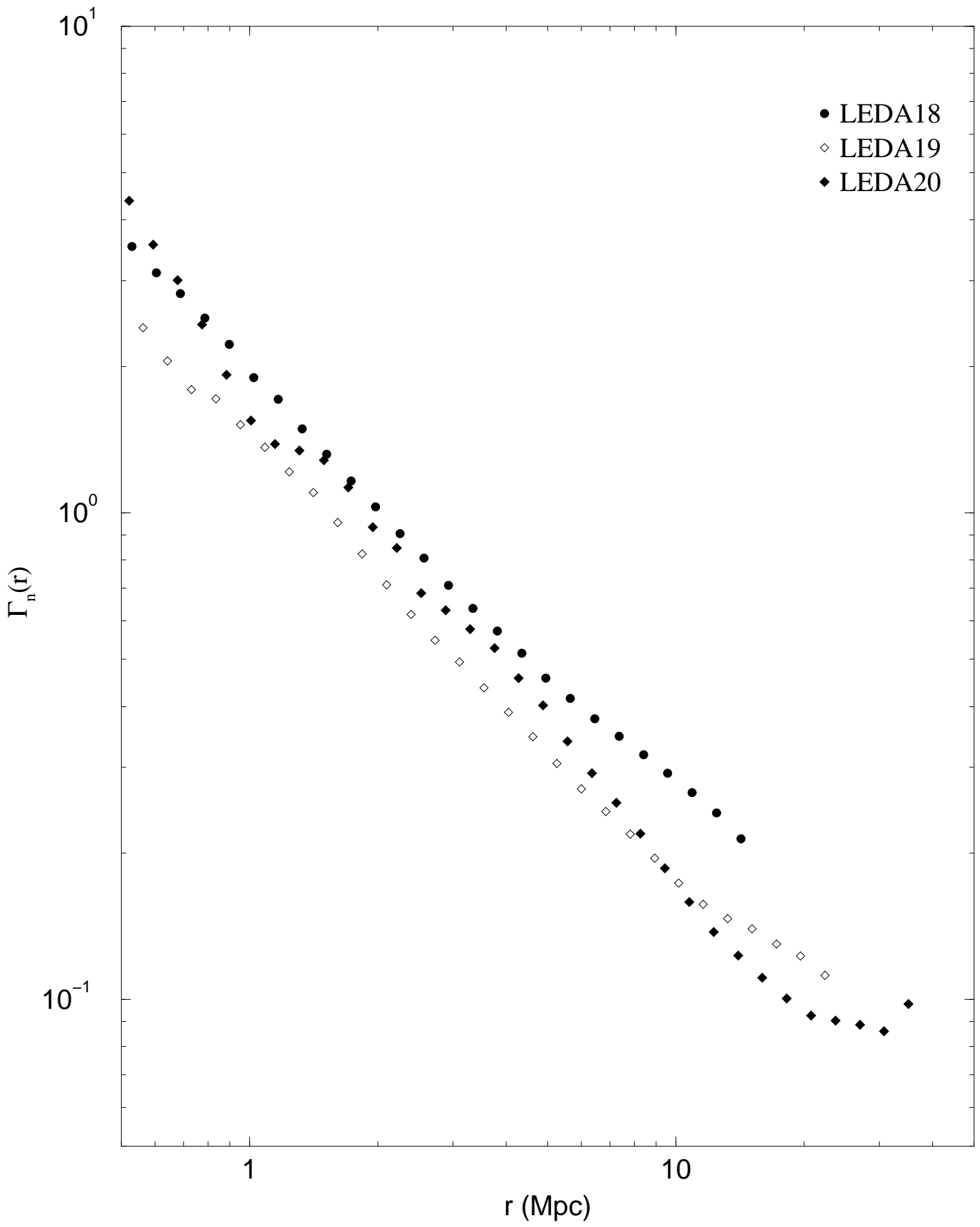


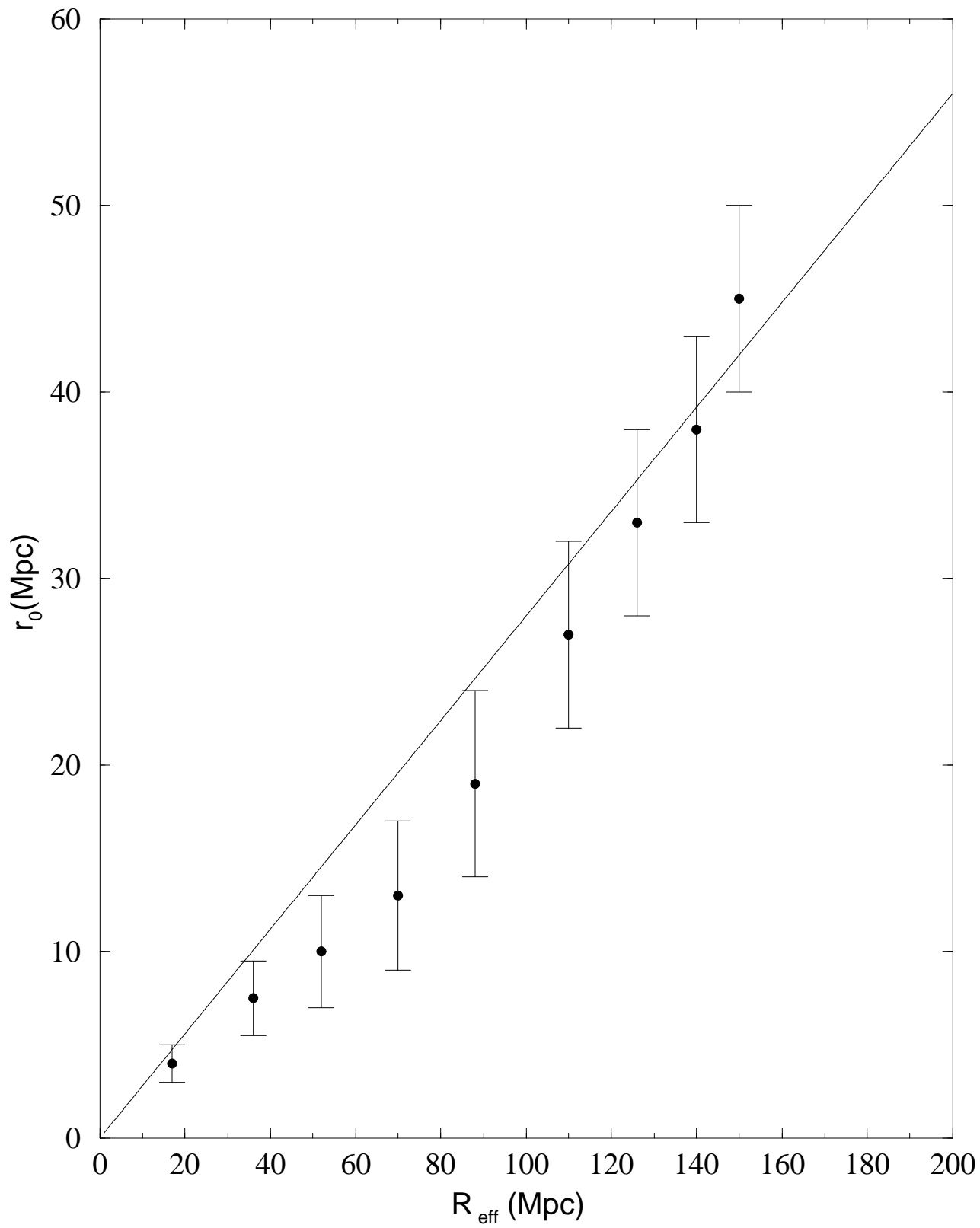












LEDA

